Performance Analysis of Hop-by-Hop Beamforming for Dual-Hop MIMO AF Relay Networks

Gayan Amarasuriya, *Student Member, IEEE*, Chintha Tellambura, *Fellow, IEEE*, and Masoud Ardakani, *Senior Member, IEEE*

***Abstract*—A comprehensive performance analysis framework for dual-hop multiple-input multiple-output (MIMO) amplify-and-forward (AF) relay networks with hop-by-hop beamforming (i.e. both source and relay perform beamforming) is presented. The system performance degradation due to practical transmission impairments (i) feedback delays, (ii) channel estimation errors and (iii) spatially-correlated fading is quantified. To this end, closed-form expressions for the cumulative distribution function of the end-to-end signal-to-noise ratio, its moment generating function, the outage probability, and the average bit error rate (BER) are derived. The asymptotic high SNR approximations of the outage probability and average BER are derived to obtain valuable system-design insights such as the diversity order and array gain. In order to illustrate the usefulness of our analysis, four applications, which employ dual-hop MIMO relaying with hop-by-hop beamforming, are also presented and analyzed. Furthermore, our analyses are validated through Monte-Carlo simulations.**

***Index Terms*—MIMO, amplify-and-forward, relay networks, beamforming.**

I. Introduction

COOPERATIVE dual-hop multiple-input multiple-output (MIMO) relay networks are being investigated for emerging wireless system standards such as IEEE 802.16m and Long Term Evolution (LTE)-Advanced [1], [2]. Such networks may employ transmit beamforming particularly because of its robustness against severe effects of fading [3]. In dual-hop MIMO relay networks, this robustness is achieved by steering the transmitted signal along the maximum eigenmodes of the source-to-relay ($S \rightarrow R$) and relay-to-destination ($R \rightarrow D$) hops. Nevertheless, a comprehensive performance analysis of hop-by-hop beamforming (i.e. both source and relay perform independent eigenmode beamforming) for dual-hop MIMO amplify-and-forward (AF) relay networks, which allows the use of all MIMO-enabled terminals and considers practical transmission impairments such as spatially-correlated fading, channel estimation errors, and feedback delays, is not available in the literature.

Prior related research: Although beamforming (a.k.a. maximal ratio transmission (MRT)) at the source has already been studied for dual-hop AF MIMO relay networks [4]–[8], these studies are limited to a single-antenna relay (R) terminal. In [4], the performance of channel-assisted AF (CA-AF) relay networks over independent Rayleigh fading channels is investigated. Reference [5] extends [4] by considering spatially-correlated fading at the source (S) and destination (D). Further, in [6], the performance of the system set-up in [4] is studied over independent Nakagami-m fading channels. Reference [7] investigates the performance of beamforming for fixed-gain AF (FG-AF) relay networks over independent Nakagami-m fading channels. In [8], the system set-up of [7] is studied over spatially-correlated Rayleigh fading channels.

In addition to the above studies, [9] analyzes the performance of dual-hop CA-AF beamforming and its equivalent systems by using several antenna configurations at S, R and D. However, in all these system set-ups, one or more terminals are limited to single antenna setups. Moreover, [10] studies the effect of multiple antennas at S on the outage probability by using MRT for the $S \rightarrow R$ channel, and [11] extends this study to investigate the effect of feedback delays on MRT beamforming. Although the system setups in [10], [11] employ multiple-antennas at S, both R and D are single-antenna terminals. References [12]–[14] study designing of MIMO precoding matrices for dual-hop MIMO relay networks by using optimization theory. In [15], a power allocation scheme is proposed for MIMO orthogonal frequency division multiplexing (OFDM) AF relay networks systems with beamforming. Moreover, in [16], beamforming is studied for improving the spatial multiplexing gains of dual-hop MIMO AF relay networks.

Motivation and our contribution: Therefore, the limitation of all the previous studies [4]–[8], [10], [11] is the presence of one or more single-antenna terminals, and beamforming is done only at the source. In other words, the most general case of all MIMO terminals where both the source and the relay perform beamforming has not been treated before. Furthermore, all the previous analyses except [11][1] make the ideal assumption of the availability of perfect CSI. In our work, this ideal assumption is replaced by more realistic one, and thus, a much more general performance analysis of beamforming in MIMO AF relay networks is presented. Specifically, the transmission strategies proposed in [12]–[14] do not provide mathematically tractable end-to-end signal-to-

Paper approved by D. J. Love, the Editor for MIMO and Adaptive Techniques of the IEEE Communications Society. Manuscript received September 29, 2010; revised August 24 and December 19, 2011.

This work has been presented in part at the IEEE Int. Conf. on Commun. (ICC), Kyoto, Japan, Jun. 2011.

The authors are with the Department of Electrical and Computer Engineering, University of Alberta, Edmonton, AB, Canada T6G 2V4 (e-mail: {amarasur, chintha, ardakani}@ece.ualberta.ca).

Digital Object Identifier 10.1109//TCOMM.2012.051012.100594

[1]The analysis in [11] is limited to feedback delay effect only on $S \rightarrow R$ for CA-AF relay networks with multiple-antenna S, and single-antenna R and D.

noise ratio (e2e SNR) expressions, and hence, no closed-form performance metrics can be derived due to heavily involved MIMO precoders at the source and relay resulted from the complex optimization problems. Further, the studies in [12]–[16] do not consider practical transmission impairments.

More specifically, in our system model, all three terminals, S, R and D, are equipped with N_s, N_r and N_d antennas, respectively. Our analysis in fact renders itself to study the detrimental impact of practical transmission impairments; (i) outdated channel state information (CSI) due to feedback delays, (ii) channel estimation errors and (iii) spatially correlated fading. The main contributions of our work can be listed as follows:

1) A mathematically tractable e2e SNR expression is derived and used to quantify the performance degradation due to aforementioned transmission impairments.
2) A general closed-form expression for the cumulative distribution function (CDF) of the e2e SNR is derived, and thereby, the outage probability is evaluated.
3) The MGF of an upper bound of the e2e SNR is derived in closed-form. A lower bound for the average bit error rate (BER) of binary phase shift keying (BPSK) is derived. These bounds are tight in the moderately low-to-high SNR regime and in fact are asymptotically exact, and hence, render them useful as benchmarks for practical system design.
4) Moreover, a unified high SNR performance analysis approach applicable to any hop-by-hop MIMO transmission scheme (i.e., beamforming, transmit antenna selection (TAS)/maximal ratio combining (MRC), transmit/receive antenna pair selection, etc.), is presented and used to obtain valuable system-design parameters such as diversity order and array gain.
5) An asymptotically exact and tight outage probability lower bound is derived by considering the arbitrarily-correlated transmit and receive correlation matrices at each terminal. In order to quantify the amount of degradation (compared to the case of the uncorrelated antennas) due to antenna correlation, the asymptotic outage probability and average BER are also derived for the correlated fading case.
6) The impact of the presence of the direct channel between the source and the destination on the system performance is studied by deriving a tight upper bound of the e2e SNR and then evaluating an accurate approximation of the average BER of BPSK.
7) In order to illustrate the usefulness of our analysis, four direct applications are presented and analyzed as well. Our results related to these applications are (i) the capacity bounds of MIMO beamforming under an adaptive transmission, (ii) high SNR performance metrics and ergodic sum-capacity of multiuser relay networks with and without opportunistic user selection, respectively, (iii) best relay selection networks, and (iv) multi-hop relay networks.

The rest of this paper is organized as follows: Section II presents the system and the channel model. In Section III, the performance analysis is presented. Section IV provides four applications of our analyses. Section V contains the numerical and simulation results. Section VI concludes the paper. The proofs are given in the Appendix.

Notations: $\mathcal{K}_\nu(z)$ is the Modified Bessel function of the second kind of order ν [17, Eq. (8.407.1)]. $\mathcal{J}_0(z)$ is the Bessel function of the first kind of order zero [17, Eq. (8.402)]. ${}_2\mathcal{F}_1(\alpha,\phi;\gamma;z)$ is the Gauss Hypergeometric function [17, Eq. (9.14.1)]. $E_n(\mu)$ is the Exponential integral of order n [17, Eq. (8.211.1)]. $\mathcal{Q}(z)$ is the Gaussian Q-function [18, Eq. (26.2.3)]. $\Re\{z\}$ is the real part of z. $\|\mathbf{Z}\|_F$ is the Frobenius norm of $\mathbf{Z}$. A circular symmetric complex Gaussian random variable with mean μ and variance σ^2 is defined by $z \sim \mathcal{CN}(\mu,\sigma^2)$. $\mathcal{E}_Z\{z\}$ is the expected value of z over the random variable Z. $\mathrm{Tr}(\mathbf{Z})$ and $[\mathbf{Z}]_{i,j}$ denote the trace and (i,j)-th element of matrix $\mathbf{Z}$.

II. System and Channel Models

We consider a dual-hop AF relay network (Fig. 1) with MIMO-enabled S, R and D having N_s, N_r and N_d antennas, respectively. The channel matrices $S \to R$ and $R \to D$ are denoted by $\mathbf{H}_1$ and $\mathbf{H}_2$. The channel coefficient from the j-th transmit antenna to the i-th receive antenna is denoted by $h_l^{i,j}$, for $l = 1, 2$ and is assumed to be independent and identically distributed Rayleigh fading unless otherwise stated[2]; $h_l^{i,j} \sim \mathcal{CN}(0,1)$. The additive noise at the terminals is modeled as complex zero mean white Gaussian noise. All the terminals operate in the half-duplex mode, and the e2e data transmission takes place in two time-slots [19]. The direct link $S \to D$ is assumed to be unavailable unless otherwise stated[3] due to impairments such as heavy shadowing and path-loss.

A. Channel state information

In practical MIMO systems, the estimated channel matrices are generally perturbed by addition of Gaussian errors due to channel estimation errors. Moreover, the beamforming vectors could be selected by using outdated CSI matrices due to feedback delays. The channel matrices with practical transmission impairments can be modeled as follows [20]–[22]:

$$\mathbf{H}_l(t) = \rho_l \hat{\mathbf{H}}_l(t-\tau_l) + \mathbf{E}_{e,l} + \mathbf{E}_{d,l}, \text{ for } l \in \{1,2\}, \quad (1)$$

where $\hat{\mathbf{H}}_l(t-\tau_l)$, for $l = 1, 2$ is the τ_l-delayed estimated channel matrix with mean zero and variance $(1-\sigma_{e,l}^2)$ Gaussian entries, and ρ_l is the normalized correlation coefficient for the τ_l-delayed feedback channel given by $\rho_l = \mathcal{E}\left\{\hat{h}_l^{i,j}(t)[\hat{h}_l^{i,j}(t-\tau_l)]^H\right\}/(1-\sigma_{e,l}^2)$. Here, $\mathbf{E}_{e,l} = \mathbf{H}_l(t) - \hat{\mathbf{H}}_l(t)$ is the channel estimation error matrix, independent with both $\hat{\mathbf{H}}_l(t)$ and $\mathbf{E}_{d,l}$, with mean zero and variance $\sigma_{e,l}^2$ Gaussian entries. The additional channel estimation errors perturbed by the feedback delay are modeled by $\mathbf{E}_{d,l} = \hat{\mathbf{H}}_l(t) - \rho_l \hat{\mathbf{H}}_l(t-\tau_l)$ with mean zero and variance $(1-\sigma_{e,l}^2)(1-\rho_l^2)$ Gaussian entries.

[2]The detrimental impact of correlated fading on the system performance is studied in Section III-E. This scenario is separately treated because the independent fading case cannot be obtained by substituting identity matrices for double-correlation matrices in (12).

[3]The effect of the direct channel on the system performance is studied separately in Section III-F as it does not lend itself to exact performance analysis.

The channel model in (1) can readily be expressed in a general form as follows:

$$\mathbf{H}_l = \vartheta_l \hat{\mathbf{H}}_l + \xi_l \mathbf{E}_l, \text{ for } l \in \{1, 2\}, \tag{2}$$

where $\mathbf{H}_l$ and $\hat{\mathbf{H}}_l$ are the actual and estimated channel matrices, and $\mathbf{E}_l$, which is independent with $\hat{\mathbf{H}}_l$, is the error matrix, and all three have zero mean and unit variance i.i.d. Gaussian entries. The parameters ϑ_l and ξ_l account for the channel estimate quality and can be explicitly given for three cases: (i) outdated CSI: $\vartheta_l = \rho_l$ and $\xi_l = \sqrt{1-\rho_l^2}$, (ii) channel estimation errors: $\vartheta_l = 1/\sqrt{1+\sigma_{e,l}^2}$ and $\xi_l = \sqrt{\sigma_{e,l}^2/(1+\sigma_{e,l}^2)}$, and (iii) both outdated CSI and channel estimation errors: $\vartheta_l = \rho_l\sqrt{1-\sigma_{e,l}^2}$ and $\xi_l = \sqrt{1-\rho_l^2+\rho_l^2\sigma_{e,l}^2}$.

B. End-to-end SNR

In the first time-slot, S transmits the symbol $\mathcal{X}$, having $\mathcal{E}\{[|\mathcal{X}|^2]\} = 1$, by employing the transmit precoding vector selected by using the imperfect CSI matrix $\hat{\mathbf{H}}_1$. Then the signal at R is combined by applying the receive filtering vector, which is again selected by using $\hat{\mathbf{H}}_1$, as

$$\begin{aligned} Y_R &= \hat{\mathbf{u}}_1^H \left[\sqrt{\mathcal{P}_1}\mathbf{H}_1\hat{\mathbf{v}}_1\mathcal{X} + \mathbf{n}_1\right] \\ &= \hat{\mathbf{u}}_1^H\left[\sqrt{\mathcal{P}_1}\left(\vartheta_1\hat{\mathbf{H}}_1 + \xi_1\mathbf{E}_1\right)\hat{\mathbf{v}}_1\mathcal{X} + \mathbf{n}_1\right] = \vartheta_1\sqrt{\mathcal{P}_1\hat{\lambda}_1}\mathcal{X} + \hat{\mathbf{n}}_R, \end{aligned} \tag{3}$$

where $\hat{\mathbf{u}}_1$ and $\hat{\mathbf{v}}_1$ are the transmit precoding and receive filtering vectors[4] at S and R, and selected by using the imperfect channel matrix $\hat{\mathbf{H}}_1$ as the first columns of $\hat{\mathbf{U}}_1$ and $\hat{\mathbf{V}}_1$, respectively, corresponding to the largest singular value of $\hat{\mathbf{H}}_1$. Here $\mathcal{P}_1$ is the transmit power at S and $\hat{\mathbf{n}}_R$ can be considered as the effective noise component having mean zero and variance $\sigma_{\hat{n}_R}^2 = \mathcal{P}_1\xi_1^2 + \sigma_1^2$ [22]. Furthermore, $\hat{\lambda}_1$ is the largest eigenvalue of the Wishart matrix $\hat{\mathbf{H}}_1^H\hat{\mathbf{H}}_1$.

In the second time-slot, R amplifies the received signal Y_R with a gain G and forwards to D again by using beamforming. The signal received at D, Y_D is thus given by

$$Y_D = \hat{\mathbf{u}}_2^H\left[G\mathbf{H}_2\hat{\mathbf{v}}_2 Y_R + \mathbf{n}_2\right] = G\vartheta_1\vartheta_2\sqrt{\mathcal{P}_1\hat{\lambda}_1\hat{\lambda}_2}\mathcal{X} + \hat{\mathbf{n}}_D, \tag{4}$$

where $\mathcal{P}_2$ is the transmit power at R and $\hat{\mathbf{n}}_D$ is the effective noise component having mean zero and variance $\sigma_{\hat{n}_D}^2 = G^2\mathcal{P}_1\hat{\lambda}_1\vartheta_1^2\xi_2^2 + G^2\hat{\lambda}_2\vartheta_2^2\sigma_{\hat{n}_R}^2 + G^2\xi_2^2\sigma_{\hat{n}_R}^2 + \sigma_2^2$ [22]. Again, the beamforming vectors $\hat{\mathbf{u}}_2$ and $\hat{\mathbf{v}}_2$ are selected by using the imperfect channel matrix $\hat{\mathbf{H}}_2$ as the first columns of $\hat{\mathbf{U}}_2$ and $\hat{\mathbf{V}}_2$. Here, $\hat{\lambda}_2$ is the largest eigenvalues of Wishart matrix $\hat{\mathbf{H}}_2\hat{\mathbf{H}}_2^H$. After some mathematical manipulations, the e2e SNR γ_{eq} can be derived as

$$\gamma_{eq} = \vartheta_1^2\mathcal{P}_1\hat{\lambda}_1\vartheta_2^2\hat{\lambda}_2/(\mathcal{P}_1\hat{\lambda}_1\vartheta_1^2\xi_2^2 + \hat{\lambda}_2\vartheta_2^2\sigma_{\hat{n}_R}^2 + \xi_2^2\sigma_{\hat{n}_R}^2 + \sigma_2^2/G^2) \tag{5a}$$

The AF relay gain in (5a) is set to $G = \sqrt{\mathcal{P}_2/(\mathcal{P}_1\hat{\lambda}_1 + \sigma_1^2)}$, and then the e2e SNR can be derived as

$$\gamma_{eq} = \gamma_1\gamma_2/(\alpha\gamma_1 + \gamma_2 + \beta), \tag{5b}$$

where $\alpha = \frac{\mathcal{P}_2\xi_2^2\vartheta_1^2+\sigma_2^2}{\vartheta_1^2(\mathcal{P}_2\xi_2^2+\sigma_2^2)}$, and $\beta = \frac{\mathcal{P}_2\xi_2^2(\mathcal{P}_1\xi_1^2+\sigma_1^2)+\sigma_1^2\sigma_2^2}{(\mathcal{P}_1\xi_1^2+\sigma_1^2)(\mathcal{P}_2\xi_2^2+\sigma_2^2)}$. Here, $\gamma_1 = \bar{\gamma}_1\hat{\lambda}_1$ and $\gamma_2 = \bar{\gamma}_2\hat{\lambda}_2$ are the instantaneous SNRs of $S \to R$ and $R \to D$ hops, where $\bar{\gamma}_1 = \mathcal{P}_1\vartheta_1^2/(\mathcal{P}_1\xi_1^2 + \sigma_1^2)$ and $\bar{\gamma}_2 = \mathcal{P}_2\vartheta_2^2/(\mathcal{P}_2\xi_2^2 + \sigma_2^2)$. Furthermore, $\hat{\lambda}_1$ and $\hat{\lambda}_2$ are the largest eigenvalues of the Wishart matrices $\hat{\mathbf{H}}_1\hat{\mathbf{H}}_1^H$ and $\hat{\mathbf{H}}_2\hat{\mathbf{H}}_2^H$, respectively.

Remark II.1: One important advantage of using hop-by-hop beamforming is that it allows resolving all available eigenmodes of both the first hop and the second hop. Although, we only consider the dominant eigenmode transmission, one could also use all the eigenmodes to improve the overall capacity. Thus, eigenmode mapping and optimal power allocation can now be performed.

III. Performance Analysis

This section presents the performance analysis. First, a general expression for the CDF of e2e SNR is derived, which is then used to derive the MGF, outage probability, and average BER. These performance metrics provide valuable insights into practical system-designs quantifying the adverse effects of the outdated CSI, and channel estimation errors. In particular, the impacts of spatially-correlated fading and presence of a source-to-destination direct channel on the system performance are studied. Moreover, in order to obtain valuable system-design parameters, such as the diversity and array gains, the asymptotic outage probability and average BER are derived.

A. Statistical characterization of the end-to-end SNR

1) CDF of the e2e SNR: The general CDF of the e2e SNR (5b) for dual-hop CA-AF relay networks with beamforming is given by (see Appendix I for the proof)

$$\begin{aligned} F_{\gamma_{eq}}(x) = 1 - &\sum_{a=1}^{\min(N_s,N_r)(N_s+N_r)a-2a^2}\ \sum_{b=|N_s-N_r|}\ \sum_{k=1}^{\min(N_r,N_d)(N_r+N_d)k-2k^2}\ \sum_{l=|N_r-N_d|} \\ &\times \sum_{m=0}^{l}\sum_{u=0}^{m}\sum_{v=0}^{b} \frac{2\alpha^u\binom{m}{u}\binom{b}{v}d_1(a,b)d_2(k,l)(k)^{\frac{u+v+m+1}{2}}}{b!\ m!(a)^{\frac{u+v-m-2b-1}{2}}} \\ &\times \frac{x^{\frac{m+2b+u-v+1}{2}}(\alpha x+\beta)^{\frac{m-u+v+1}{2}}}{(\bar{\gamma}_1)^{\frac{2b-u-v+m+1}{2}}(\bar{\gamma}_2)^{\frac{u+v+m+1}{2}}}\ \mathrm{e}^{-x\left(\frac{a}{\bar{\gamma}_1}+\frac{\alpha k}{\bar{\gamma}_2}\right)} \\ &\times \mathcal{K}_{u+v-m+1}\left(2\sqrt{akx(\alpha x+\beta)/(\bar{\gamma}_1\bar{\gamma}_2)}\right), \end{aligned} \tag{6}$$

where the coefficients[5] $d_l(i,j)|_{l=1}^2$ satisfy $d_l(i,j) = \sum_{i=1}^{\min(N,M)}\sum_{j=|N-M|}^{(N+M)i-2i^2} d_l(i,j) = 1$ and can readily be computed by using the efficient algorithm in [23].

2) MGF of the e2e SNR: The MGF is a useful statistic, which can be used efficiently for unified performance analysis. The MGF of an asymptotically exact upper bound of the e2e

[4]The singular value decompositions of $\hat{\mathbf{H}}_1$ and $\hat{\mathbf{H}}_2$ are given by $\hat{\mathbf{H}}_1 = \hat{\mathbf{U}}_1\hat{\mathbf{\Sigma}}_1\hat{\mathbf{V}}_1^H$ and $\hat{\mathbf{H}}_2 = \hat{\mathbf{U}}_2\hat{\mathbf{\Sigma}}_2\hat{\mathbf{V}}_2^H$. Here $\hat{\mathbf{\Sigma}}_1$ and $\hat{\mathbf{\Sigma}}_2$ are $N_r \times N_s$ and $N_d \times N_r$ matrices having the largest singular values $\sqrt{\lambda_1}$ and $\sqrt{\lambda_2}$, as the first elements on the main diagonals, respectively. Further, $\hat{\mathbf{U}}_1$, $\hat{\mathbf{V}}_1$, $\hat{\mathbf{U}}_2$ and $\hat{\mathbf{V}}_2$ are unitary square matrices of sizes $N_r \times N_r$, $N_s \times N_s$, $N_d \times N_d$, and $N_r \times N_r$.

[5]In fact, $d_l(i,j)|_{l=1}^2$ is the coefficient of the term $\mathrm{e}^{-ix}x^j$ in the expansion of $\frac{d}{dx}[\mathcal{S}_l(x)]$, where $\mathcal{S}_l(x)$ is an $a_l \times a_l$ Hankel matrix with elements given by $\mathcal{S}_l^{(i,j)}(x) = \gamma(b_l - a_l + i + j - 1, x)$. Here, $a_1 = \min(N_s, N_r)$, $a_2 = \min(N_r, N_d)$, $b_1 = \max(N_s, N_r)$, and $b_2 = \max(N_r, N_d)$ [22].

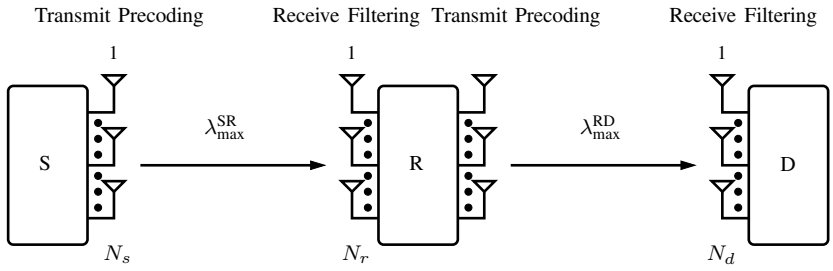

Fig. 1. Hop-by-hop beamforming for a MIMO AF relay network

SNR is thus derived as (see Appendix II for the proof)

$$\mathcal{M}_{\gamma_{eq}^{ub}}(s) = 1 - \sum_{a,b,k,l,m} \sum_{u=0}^{m+b} \frac{2\binom{m+b}{u} d_1(a,b) d_2(k,l)}{b!\, m! (a)^{\frac{u-m-2b-1}{2}}} \times \frac{(\alpha k)^{\frac{u+m+1}{2}}}{(\bar{\gamma}_1)^{\frac{2b-u+m+1}{2}} (\bar{\gamma}_2)^{\frac{u+m+1}{2}}} \mathbb{J}_{\mu,\nu,\psi,\omega}(s), \quad (7a)$$

where the function $\mathbb{J}_{\mu,\nu,\psi,\omega}(s)$ is given by

$$\mathbb{J}_{\mu,\nu,\psi,\omega}(s) = \frac{\sqrt{\pi}(2\omega)^{\nu} \Gamma(\mu+\nu)\,\Gamma(\mu-\nu)}{(\psi+\omega)^{\mu+\nu}\,\Gamma\left(\mu+\frac{1}{2}\right)} \times s\, {}_2\mathcal{F}_1\left(\mu+\nu, \nu+\frac{1}{2}; \mu+\frac{1}{2}; \frac{\psi-\omega}{\psi+\omega}\right). \quad (7b)$$

In (7a), $\sum_{a,b,k,l,m} = \sum_{a=1}^{\min(N_s,N_r)} \sum_{b=|N_s-N_r|}^{(N_s+N_r)a-2a^2} \sum_{k=1}^{\min(N_r,N_d)} \sum_{l=|N_r-N_d|}^{(N_r+N_d)k-2k^2} \sum_{m=0}^{l}$, $\mu = m+b+2$, $\nu = u-m+1$, $\psi = s + a/\bar{\gamma}_1 + \alpha k/\bar{\gamma}_2$, and $\omega = 2\sqrt{a\alpha k/(\bar{\gamma}_1\bar{\gamma}_2)}$.

The probability density function (PDF) of γ_{eq} can readily be derived by differentiating the CDF in (6) with respect to x by using [17, Eq. (8.486.12)]. Further, the generalized SNR moments $\overline{\gamma_{eq}^n} = \mathcal{E}\{\gamma_{eq}^n\}$ can also be derived by substituting (6) into $\overline{\gamma_{eq}^n} = \int_0^\infty n x^{n-1}\left(1 - F_{\gamma_{\text{eq}}}(x)\right) \mathrm{d}x$ and by solving the integral by using [17, Eqs. (6.621.3) and (6.643.3)]. However, for the sake of brevity, the PDF and SNR moment results are omitted.

B. Outage probability

The SNR outage probability[6] is the probability that the instantaneous e2e SNR, γ_{eq}, falls below a threshold γ_{th}. The outage probability, P_{out}, can thus be obtained as $P_{out} = \Pr(\gamma_{eq} \le \gamma_{th}) = F_{\gamma_{eq}}(\gamma_{th})$, where $F_{\gamma_{eq}}(\gamma_{th})$ denotes the CDF of γ_{eq} (6) evaluated at γ_{th}.

C. Average bit error rate of BPSK

In this section, a tight lower bound of the average BER of BPSK is derived in closed-form. The receive signal, which is post-processed by using the imperfect CSI matrices at the destination is given by (4) and re-written as

$$Y_D = \hat{\mathbf{u}}_2^H \left[G\mathbf{H}_2\hat{\mathbf{v}}_2 Y_R + \mathbf{n}_2\right] = G\vartheta_1\vartheta_2\sqrt{\mathcal{P}_1\hat{\lambda_1}\hat{\lambda}_2}\mathcal{X} + \hat{\mathbf{n}}_D,$$

where $\hat{\mathbf{n}}_D$ is the effective noise component and is assumed to be distributed as $\hat{\mathbf{n}}_D|_{\hat{\lambda}_1,\hat{\lambda}_2} \sim \mathcal{CN}(0, \sigma^2_{\hat{n}_D})$, where $\sigma^2_{\hat{n}_D} = G^2\mathcal{P}_1\hat{\lambda}_1\vartheta_1^2\xi_2^2 + G^2\hat{\lambda}_2\vartheta_2^2\sigma^2_{\hat{n}_R} + G^2\xi_2^2\sigma^2_{\hat{n}_R} + \sigma_2^2$ and $\sigma^2_{\hat{n}_R} = \mathcal{P}_1\xi_1^2 + \sigma_1^2$.

The BER of BPSK conditioned on $\hat{\lambda}_1$ and $\hat{\lambda}_2$ can be derived as follows:

$$P_e|_{\hat{\lambda}_1,\hat{\lambda}_2} = \Pr\left(\Re\left(Y_D\right) < 0 | \mathcal{X} = 1\right)\Pr\left(\mathcal{X}=1\right) + \Pr\left(\Re\left(Y_D\right) > 0 | \mathcal{X} = -1\right)\Pr\left(\mathcal{X}=-1\right). \quad (8a)$$

By assuming that the symbols are drawn equiprobably, conditional BER can be further simplified as

$$P_e|_{\hat{\lambda}_1,\hat{\lambda}_2} = \Pr\left(\Re\left(Y_D\right) < 0 | \mathcal{X} = 1\right) \quad (8b)$$

Now, $\Re(Y_D)$ is a Gaussian random variable with mean $G\vartheta_1\vartheta_2\sqrt{\mathcal{P}_1\hat{\lambda}_1\hat{\lambda}_2}$ and variable $\frac{\sigma^2_{\hat{n}_D}}{2}$. Thus, $P_e|_{\hat{\lambda}_1,\hat{\lambda}_2}$ can be alternatively presented as

$$P_e|_{\hat{\lambda}_1,\hat{\lambda}_2} = \mathcal{Q}\left(\sqrt{2G^2\vartheta_1^2\vartheta_2^2\mathcal{P}_1\hat{\lambda}_1\hat{\lambda}_2/\sigma^2_{\hat{\mathbf{n}}_D}}\right). \quad (8c)$$

By using (5a) and (5b), the argument inside $\mathcal{Q}(\cdot)$ can be further simplified as

$$P_e|_{\hat{\lambda}_1,\hat{\lambda}_2} = \mathcal{Q}\left(\sqrt{\bar{\gamma}_1\hat{\lambda}_1\bar{\gamma}_2\hat{\lambda}_2/(\alpha\bar{\gamma}_1\hat{\lambda}_1 + \bar{\gamma}_2\hat{\lambda}_2 + \beta)}\right) = \mathcal{Q}\left(\sqrt{2\gamma_{eq}}\right), \quad (8d)$$

where α , β and γ_{eq} are defined in (5b).

An asymptotically exact and tight lower bound of the average BER of BPSK can be derived (see Appendix III for the proof)

$$\bar{P}_e^{lb} = \frac{1}{2} - \frac{1}{2}\sum_{a,b,k,l,m}\sum_{u=0}^{m+b} \frac{2\binom{m+b}{u} d_1(a,b) d_2(k,l)}{b!\, m! (a)^{\frac{u-m-2b-1}{2}}} \times \frac{(\alpha k)^{\frac{u+m+1}{2}}}{(\bar{\gamma}_1)^{\frac{2b-u+m+1}{2}} (\bar{\gamma}_2)^{\frac{u+m+1}{2}}} \mathbb{I}(\mu,\nu,\psi,\omega), \quad (9a)$$

In (9a), $\mathbb{I}(\mu,\nu,\psi,\omega)$ is defined as

$$\mathbb{I}(\mu,\nu,\psi,\omega) = \frac{\sqrt{\pi}(2\omega)^{\nu}\Gamma(\mu+\nu)\,\Gamma(\mu-\nu)}{(\psi+\omega)^{\mu+\nu}\,\Gamma\left(\mu+\frac{1}{2}\right)} \times {}_2\mathcal{F}_1\left(\mu+\nu, \nu+\frac{1}{2}; \mu+\frac{1}{2}; \frac{\psi-\omega}{\psi+\omega}\right), \quad (9b)$$

where $\mu = m+b+3/2$, $\nu = u-m+1$, $\psi = 1+a/\bar{\gamma}_1+\alpha k/\bar{\gamma}_2$, and $\omega = 2\sqrt{a\alpha k/(\bar{\gamma}_1\bar{\gamma}_2)}$.

D. High SNR analysis

In this section, the asymptotic performance metrics for the perfect CSI case ($\rho_l = 1$ and $\sigma_{e,l} = 0$) are derived in order to obtain valuable system-design parameters such as the diversity order (G_d) and array gain (G_a). These analytic expressions in fact, render themselves to quantify the amount of performance degradation due to the impact of outdated CSI,

[6]The information outage probability can be defined as the probability that the instantaneous mutual information $\mathcal{I}$ falls below the target rate $\mathcal{R}_{th}$; $\Pr(\mathcal{I} = \frac{1}{2}\log(1+\gamma_{\text{eq}}) \le \mathcal{R}_{th}) = F_{\gamma_{\text{eq}}}(\gamma_{th})$, where $\gamma_{th} = 2^{2\mathcal{R}_{th}} - 1$.

channel estimation errors and spatially correlated fading with respect to perfect CSI case.

1) Asymptotic outage probability: As a direct insight of our analysis, the asymptotic outage probability can be derived as (see Appendix IV for the proof)

$$P_{out}^{\infty}=\Omega\left(\gamma_{th}/\bar{\gamma}\right)^{G_d}+o\left(\bar{\gamma}^{-(G_d+1)}\right), \tag{10a}$$

where $G_d = N_r \min(N_s, N_d)$ and Ω is given by

$$\Omega=\begin{cases}\frac{\Gamma_{n_1}(n_1)}{\Gamma_{n_1}(m_1+n_1)k_1^{N_sN_r}}, & N_s<N_d\\ \frac{\Gamma_{n_1}(n_1)}{\Gamma_{n_1}(m_1+n_1)k_1^{NN_r}}+\frac{\Gamma_{n_2}(n_2)}{\Gamma_{n_2}(m_2+n_2)k_2^{NN_r}}, & N_s=N_d=N\\ \frac{\Gamma_{n_2}(n_2)}{\Gamma_{n_2}(m_2+n_2)k_2^{N_dN_r}}, & N_s>N_d.\end{cases} \tag{10b}$$

In (10b), $\Gamma_a(b)=\prod_{i=1}^{a}\Gamma(b-i+1)$ is the normalized complex multivariate gamma function. Further, $m_1=\max(N_s,N_r)$, m_2=$\max(N_r,N_d)$, n_1=$\min(N_s,N_r)$, and n_2=$\min(N_r,N_d)$.

2) Asymptotic average BER : At high SNRs, the average BER of BPSK can be approximated as $\bar{P}_e^{\infty}\approx(\bar{\gamma}G_a)^{-G_d}$, where G_d is the diversity order, and G_a is the array gain [24]. By using (10a) and the integral expression of $\bar{P}_e$ in Section III-C, the asymptotic average BER is derived as

$$\bar{P}_e^{\infty}=\frac{\Omega\Gamma(G_d+\frac{1}{2})}{2\sqrt{\pi}(\bar{\gamma})^{G_d}}+o\left(\bar{\gamma}^{-(G_d+1)}\right). \tag{11a}$$

Now, by using (10a) and (11a), the diversity order and array gain can be obtained as

$$G_d=N_r\min(N_s,N_d) \text{ and } G_a=\left[\Omega\Gamma(G_d+1/2)/(2\sqrt{\pi})\right]^{\frac{-1}{G_d}}. \tag{11b}$$

E. Impact of correlated fading among antenna elements

In this subsection, the impact of correlated fading among the antenna elements of S, R and D on the system performance is investigated[7]. Assume that $\mathbf{H}_1$ and $\mathbf{H}_2$ undergo flat spatially arbitrary-correlated Rayleigh fading. Then $\mathbf{H}_1$ and $\mathbf{H}_2$ can be decomposed according to the Kronecker correlation structure as follows: $\mathbf{H}_1=\Upsilon_1^{\frac{1}{2}}\tilde{\mathbf{H}}_1\Phi_1^{\frac{1}{2}}$ and $\mathbf{H}_2=\Upsilon_2^{\frac{1}{2}}\tilde{\mathbf{H}}_2\Phi_2^{\frac{1}{2}}$, where Υ_1 and Υ_2 are the transmit correlation matrices at S and R, and Φ_1 and Φ_2 are the receive correlation matrices at R and D, respectively. Further, $\tilde{\mathbf{H}}_1\sim\mathcal{CN}(\mathbf{0}_{N_r\times N_r},\mathbf{I}_{N_r}\otimes\mathbf{I}_{N_s})$ and $\tilde{\mathbf{H}}_2\sim\mathcal{CN}(\mathbf{0}_{N_d\times N_r}\mathbf{I}_{N_d}\otimes\mathbf{I}_{N_r})$.

1) CDF of the e2e SNR: The exact CDF of the e2e SNR is mathematically intractable. However, the CDF of an upper bound of the e2e SNR, which is asymptotically exact at high SNRs, can be derived. By using the SNR upper bound, $\gamma_{eq}\le\gamma_{eq}^{\text{ub}}=\min(\gamma_1,\gamma_2)$ [25], [26], the CDF of γ_{eq}^{ub} can be derived as $F_{\gamma_{eq}^{\text{ub}}}(x)=F_{\gamma_1}(x)+F_{\gamma_2}(x)-F_{\gamma_1}(x)\,F_{\gamma_2}(x)$, where $F_{\gamma_1}(x)$ and $F_{\gamma_2}(x)$ are the CDFs of the first and second hop SNRs and given by [27]

$$F_{\gamma_l}(x)=\frac{(-1)^{n_l}\Gamma_{n_l}(n_l)\det(\Upsilon_l)^{n_1-1}\det(\Phi_l)^{m_1-1}\det\left(\Psi_l\left(\frac{x}{\gamma_l}\right)\right)}{\Delta_{n_l}(\Upsilon_l)\Delta_{m_l}(\Phi_l)\,(x/\gamma_l)^{n_l(n_l-1)/2}}, \tag{12}$$

where $\Delta_k(\cdot)$ is a Vandermonde determinant in the eigenvalues of the k-dimensional matrix argument, and the (i,j)-th element of $\Psi_l(x)$ is given by [27, Eq. (1)]. By evaluating $F_{\gamma_{eq}^{\text{ub}}}(x)$ at γ_{th}, a tight outage probability lower bound can readily be derived.

Specifically, this outage probability lower bound is significantly tight in medium-to-high SNR regime, and in fact, is asymptotically-exact at high SNRs [26]. Thus it serves as an accurate benchmark for exact outage analysis of practical systems (please refer to Fig. 5 for more details).

2) High SNR analysis: To quantify the amount of performance degradation due spatially correlated fading, the asymptotic outage probability and average BER are derived. By following similar steps to those in Section III-D, the asymptotic outage probability, when each channel undergoes correlated fading, can be derived by replacing Ω in (10a) with

$$\Omega'=\begin{cases}\frac{\Gamma_{n_1}(n_1)}{\det(\Upsilon_1)^{m_1}\det(\Psi_1)^{n_1}\Gamma_{n_1}(m_1+n_1)k_1^{N_sN_r}}, & N_s<N_d\\ \frac{\Gamma_{n_1}(n_1)}{\det(\Upsilon_1)^{m_1}\det(\Psi_1)^{n_1}\Gamma_{n_1}(m_1+n_1)k_1^{NN_r}}\\ +\frac{\Gamma_{n_2}(n_2)}{\det(\Upsilon_2)^{m_2}\det(\Psi_2)^{n_2}\Gamma_{n_2}(m_2+n_2)(k_2)^{NN_r}}, & N_s=N_d=N\\ \frac{\Gamma_{n_2}(n_2)}{\det(\Upsilon_2)^{m_2}v\det(\Psi_2)^{n_2}\Gamma_{n_2}(m_2+n_2)k_2^{N_dN_r}}, & N_s>N_d.\end{cases} \tag{13}$$

The asymptotic average BER can readily be derived again by substituting the above Ω_1', Ω_2' and Ω_3' into (11a). Although the diversity order of the system remains the same (i.e., $G_d'=N_r\min(N_s,N_d)$) regardless of the amount of correlation, the array gain significantly reduces with respect to the uncorrelated fading by a factor of Ω/Ω'.

F. The effect of direct channel

In this subsection, the impact of the direct channel between the source and the destination on the performance of hop-by-hop beamforming for dual-hop MIMO AF relay networks is studied. We consider same system model as in Fig. 1, but in the first time-slot, the source transmits its signal to both the relay and the destination by using a common transmit precoding (beamforming) vector. In the second time-slot, the relay transmits an amplified version of its received signal to the destination again by using the beamforming vector. By following similar steps to [12, Eq. (23)] and taking into account the imperfect CSI matrices, the e2e SNR can be derived as

$$\gamma_{eq}=\gamma_{SD}+\gamma_{SRD}, \tag{14}$$

where the effective SNRs of the direct-path and the relayed-path are given by $\gamma_{SD}=\mathcal{P}_0\vartheta_0^2||H_0\hat{v}||^2/(\mathcal{P}_0\xi_2^0+\sigma_0^2)$ and $\gamma_{SRD}=\gamma_1\gamma_2/(\alpha\gamma_1+\gamma_2^*+\beta)$, respectively. Here, $\gamma_1=\mathcal{P}_1\vartheta_1^2||H_1\hat{v}||^2/(\mathcal{P}_1\xi_2^1+\sigma_1^2)$ and $\gamma_2^*=\mathcal{P}_2\vartheta_2^2\hat{\lambda}_2/(\mathcal{P}_2\xi_2^2+\sigma_2^2)$, where α, β, σ_2, ϑ_2, ξ_2, and $\hat{\lambda}_2$ are defined in (2) and (5b).

Now the design objective is to maximize the e2e SNR (14) by choosing the optimal transmit precoding vector $\hat{v}$. Unfortunately, it does not appear to have an analytic solution for optimal $\hat{v}$. However, in [12, Eqs. (24)-(26)], a similar problem has been solved numerically as follows: the optimal $\hat{v}$ can be expressed as

$$\hat{v}^*=\underset{||\hat{v}||=1}{\text{argmax}}\frac{||H_1\hat{v}||^2}{\alpha||H_1\hat{v}||^2+\frac{\beta+\gamma_2^*}{\mathcal{P}_1}}+\frac{\mathcal{P}_0}{\gamma_2^*}||H_0\hat{v}||^2. \tag{15}$$

The maximum e2e SNR, which is obtained by substituting the optimal $\hat{v}$, can be written as

$$\gamma_{eq}^*=\gamma_0^*+\gamma_1^*\gamma_2^*/(\alpha\gamma_1^*+\gamma_2^*+\beta), \tag{16}$$

where $\gamma_0^*=\mathcal{P}_0||H_0\hat{v}^*||^2$, $\gamma_1^*=\mathcal{P}_1||H_1\hat{v}^*||^2$, and $\hat{\gamma}_2^*$ is defined

[7]Eq. (12) does not hold valid whenever the eigenvalues of the correlation matrices are all equal. Due to this reason, the impact of correlated fading case is separately treated, because the independent fading case cannot be directly obtained from (12).

in (14). The e2e SNR in (16) does not render itself to exact analytic outage and average BER expressions because the optimal $\hat{v}$ (i.e., $\hat{v}^*$) is in fact can only be evaluated numerically. As a remedy, we derive the MGF of an upper bound of the e2e SNR in closed-form, and thereby, obtain average BER, its high SNR approximation, array gain and diversity order.

1) Upper bound of the e2e SNR with direct channel: Let us assume that three time-slots are used instead of traditional two time-slot system model described in Section III-F. Thus, in the first time-slot, the source transmits by using the transmit precoding vector and the destination receives by using the receive filtering vector[8]. These two vectors are the right and left dominant singular vectors of the channel matrix between the source and the destination. Similarly, in the second[9] and third time-slots, source-relay and relay-destination transmission is performed again by using beamforming. Finally, the destination combines two independent signals received in the first and the third time-slots by using the corresponding MMSE (a.k.a weighted MRC) coefficients.

By following similar steps to those in Section II, the e2e SNR of the aforementioned system model can readily be derived as

$$\gamma_{eq}^{\text{approx}} = \gamma_0 + \gamma_1\gamma_2/(\alpha\gamma_1 + \gamma_2 + \beta), \tag{17}$$

where $\gamma_0 = \frac{\mathcal{P}_0 v_0^2 \hat{\lambda}_0}{\mathcal{P}_0\xi_0^2+\sigma_0^2}$, $\gamma_1 = \frac{\mathcal{P}_1 v_1^2 \hat{\lambda}_1}{\mathcal{P}_1\xi_1^2+\sigma_1^2}$ and $\gamma_2 = \frac{\mathcal{P}_2 v_2^2 \hat{\lambda}_2}{\mathcal{P}_2\xi_2^2+\sigma_2^2}$.

It can be clearly seen that the e2e SNR in (17) provides a tight upper bound for the e2e SNR of the optimal system model, γ_{eq}^*, given in (16). Thus, we claim the aforementioned relationship as follows:

$$\gamma_{eq}^* = \gamma_0^* + \frac{\gamma_1^*\gamma_2^*}{\alpha\gamma_1^* + \gamma_2^* + \beta} \leq \gamma_0 + \frac{\gamma_1\gamma_2}{\alpha\gamma_1 + \gamma_2 + \beta} = \gamma_{eq}^{ub}. \tag{18}$$

2) The exact MGF of the upper bound of the e2e SNR with direct channel: In this section, the MGF of the upper bound of the e2e SNR with the direct path is derived in closed-form. To this end, the PDF of the SNR of the direct channel, i.e., γ_0 in (18), is derived by using the statistics of the largest eigenvalue of central Whishart matrices [3], [22] as follows:

$$f_{\gamma_0}(x) = \sum_{c=1}^{\min(N_s,N_d)} \sum_{d=|N_s-N_d|}^{(N_s+N_d)c-2c^2} \frac{c^{d+1} d_0(c,d)}{(\bar{\gamma}_1)^{d+1}\,(d)!} x^d \mathrm{e}^{-\frac{cx}{\bar{\gamma}_0}}. \tag{19}$$

The MGF of γ_0 can be readily obtained by evaluating $\mathcal{M}_{\gamma_0}(s) = \int_0^\infty f_{\gamma_0}(x)\,\mathrm{e}^{-sx}\mathrm{d}x$ as

$$\mathcal{M}_{\gamma_0}(s) = \sum_{c=1}^{\min(N_s,N_d)} \sum_{d=|N_s-N_d|}^{(N_s+N_d)c-2c^2} \frac{c^{d+1} d_0(c,d)}{(\bar{\gamma}_0)^{d+1}} \left(s + \frac{c}{\bar{\gamma}_0}\right)^{-(d+1)} \tag{20}$$

The MGF of the relayed-channel SNR, $\gamma_{SRD} = (\gamma_1\gamma_2/(\alpha\gamma_1 + \gamma_2 + \beta)$, with $\beta = 0$ has already been derived in (7a). Now, the MFG of the upper bound of the e2e SNR with the direct path, γ_{eq}^{ub}, can readily be derived by substituting (20) and (7a) into $\mathcal{M}_{\gamma_{eq}^{ub}}(s) = \mathcal{M}_{\gamma_0}(s)\,\mathcal{M}_{\gamma_{SRD}}(s)$.

3) Average BER with direct channel: The conditional error probability (CEP) of BPSK can also be expressed in an alternative form [28]: $P_e|\gamma = \mathcal{Q}(\sqrt{2\gamma}) = \frac{1}{\pi}\int_0^\infty \exp(-\gamma(s^2+1))/(s^2+1)ds$. By using the variable transformation $s^2 + 2 = 2/(\gamma+1)$, the average BER can be written as $\bar{P}_e = \frac{1}{\pi}\int_0^\infty \mathcal{M}_{\gamma_{\text{eq}}^{ub}}(s^2+1))/(s^2+1)ds = \frac{1}{2\pi}\int_{-1}^{1} \mathcal{M}_{\gamma_{\text{eq}}^{ub}}(2/(\gamma+1))/(\sqrt{1-\gamma^2})d\gamma$ [28]. Then we use the accurate and computationally efficient method proposed in [28], which uses the Gauss-Chebyshev approximation [18] to obtain a compact closed-form approximation for the average BER as follows:

$$\bar{P}_e^{\text{approx}} = \frac{1}{2N_p}\sum_{k=1}^{N_p} \mathcal{M}_{\gamma_{\text{eq}}^{ub}}\left(\sec^2(\theta_k)\right) + R_{N_p}, \tag{21}$$

where N_p is a small positive integer, $\theta_k = (2k-1)\pi/4N_p$, and R_{N_p} is the remainder term. R_{N_p} becomes negligible as N_p increases, even for small values such as 10.

4) High SNR approximation of average BER: In order to determine the impact of the direct channel more insightfully, the asymptotic average BER of BPSK at high SNR is derived, and thereby, the diversity order and array gain are quantified as follows (see Appendix V for the proof):

$$\bar{P}_e^{\infty} = \Delta\Omega^{''}\Gamma\left(G_d^{''}+1/2\right)/(2\sqrt{\pi}(\bar{\gamma})^{G_d^{''}}) + o\left(\bar{\gamma}^{-(G_d^{''}+1)}\right), \tag{22a}$$

where Δ and $\Omega^{''}$ are given by

$$\Delta = \begin{cases} \frac{\Gamma(N_sN_d+1)\Gamma(N_sN_r+1)}{\Gamma(N_s(N_r+N_d)+1)}, & N_s < N_d \\ \frac{\Gamma(N^2+1)\Gamma(NN_r+1)}{\Gamma(N(N_r+N)+1)}, & N_s = N_d = N \\ \frac{\Gamma(N_sN_d+1)\Gamma(N_dN_r+1)}{\Gamma(N_d(N_s+N_r)+1)}, & N_s > N_d \end{cases} \tag{22b}$$

$$\Omega^{''} = \begin{cases} \frac{\Gamma_{n_0}(n_0)\Gamma_{n_1}(n_1)}{\Gamma_{n_0}(m_0+n_0)\Gamma_{n_1}(m_1+n_1)(k_0)^{N_sN_d}k_1^{N_sN_r}}, & N_s < N_d \\ \frac{\Gamma_{n_0}(n_0)}{\Gamma_{n_0}(m_0+n_0)k_0^{N^2}}\left[\frac{\Gamma_{n_1}(n_1)}{\Gamma_{n_1}(m_1+n_1)k_1^{NN_r}} + \frac{\Gamma_{n_2}(n_2)}{\Gamma_{n_2}(m_2+n_2)k_2^{NN_r}}\right], & N_s = N_d = N \\ \frac{\Gamma_{n_0}(n_0)\Gamma_{n_2}(n_2)}{\Gamma_{n_0}(m_0+n_0)\Gamma_{n_2}(m_2+n_2)k_0^{N_sN_d}k_2^{N_dN_r}}, & N_s > N_d. \end{cases} \tag{22c}$$

By using (22a), the diversity order and array gain can be readily quantified as

$$G_d^{''} = N_sN_d + N_r\min(N_s,N_d) \text{ and } G_a^{''} = \left(\frac{\Delta\Omega^{''}\Gamma(G_d^{''}+\frac{1}{2})}{2\sqrt{\pi}}\right)^{\frac{-1}{G_d^{''}}} \tag{22d}$$

IV. Applications

In this section, four applications, which employ MIMO hob-by-hop beamforming, are presented. Specifically, our analyses in Section III are used to study the performance of adaptive transmission, multiuser relay networks, best relay selection networks, and multi-hop networks.

A. Adaptive transmission with beamforming

In practice, a local feedback channel from the receiver to the transmitter is employed for transmit beamforming. The performance of such systems can be further improved by using this feedback channel for adaptive transmission as well [29]. In this section, three channel capacity upper bounds are derived for (i) optimal power and rate adaptation, (ii) optimal rate adaptation with constant transmit power, and (iii) channel inversion with fixed rate.

1) Optimal power and rate adaptation: The channel capacity under the optimal rate and power adaptation is given by $C_{\text{OPRA}} = \frac{B}{2\ln(2)}\int_{\gamma_0}^\infty \ln(x/\gamma_0)\, f_{\gamma_{eq}}(x)\,\mathrm{d}x$ [30, Eq. (7)], where B is the channel bandwidth, and γ_0 is the optimal cutoff SNR

[8]During the first time-slot, the relay remains idle.

[9]During the second time-slot, the destination remains idle.

below which the transmission is stopped. By using the PDF of an e2e SNR upper bound $f_{\gamma_{eq}^{ub}}(x)$, a tight capacity upper bound is derived as (see Appendix VI for the proof)

$$C_{\text{OPRA}}^{ub} = \frac{B}{2\ln 2} \sum_{a,b,c,k,l,m} \frac{d_1(a,b)d_2(k,l)\gamma_0^{c+m+1}a^c k^m}{(c)!\,(m)!\bar{\gamma}_1^c\bar{\gamma}_2^m} \times \left(\phi\gamma_0\mathcal{J}_{c+m+1}(\phi\gamma_0) - (c+m)\mathcal{J}_{c+m}(\phi\gamma_0)\right), \quad (23)$$

where $\sum_{a,b,c,k,l,m} = \sum_{a=1}^{\min(N_s,N_r)} \sum_{b=|N_s-N_r|}^{(N_s+N_r)a-2a^2} \sum_{c=0}^{b} \sum_{k=1}^{\min(N_r,N_d)} \sum_{l=|N_r-N_d|}^{(N_r+N_d)k-2k^2} \sum_{m=0}^{l}$, $\phi = a/\bar{\gamma}_1 + k/\bar{\gamma}_2$ and $\mathcal{J}_n(\mu) = \Gamma(n)\mu^{-n}\sum_{j=0}^{n-1}\Gamma(j,\mu)/(j)!$. The optimal cutoff SNR satisfies $\int_{\gamma_0}^{\infty}(1/\gamma_0 - 1/x) f_{\gamma_{eq}^{ub}}(x)\,\mathrm{d}x = 1$ [30, Eq. (8)] and can be estimated numerically (see Appendix VI).

2) Optimal rate adaptation with constant transmit power: The channel capacity under rate adaptation with constant transmit power is given by $C_{\text{ORA}} = \frac{B}{2\ln(2)}\int_0^{\infty}\ln(1+x)f_{\gamma_{eq}}(x)\,\mathrm{d}x$ [30, Eq. (29)]. In fact, C_{ORA} is the ergodic capacity with full CSI at the destination. Again, by using $f_{\gamma_{eq}^{ub}}(x)$, a tight capacity upper bound is derived by using [17, 3.383.10] as

$$C_{\text{ORA}}^{ub} = \frac{B}{2\ln 2} \sum_{a,b,k,l} \Bigg(\Theta_1 \mathcal{I}_1(\phi) - \sum_{c=1}^{b} \Theta_2 \left(c\mathcal{I}_c(\phi) - \phi\mathcal{I}_{c+1}(\phi)\right) - \sum_{m=1}^{l} \Theta_3 \left(m\mathcal{I}_m(\phi) - \phi\mathcal{I}_{m+1}(\phi)\right) - \sum_{c=1}^{b}\sum_{m=1}^{l} \Theta_4 \left((c+m)\mathcal{I}_{c+m}(\phi) - \phi\mathcal{I}_{c+m+1}(\phi)\right) \Bigg), \quad (24)$$

where $\sum_{a,b,k,l} = \sum_{a=1}^{\min(N_s,N_r)} \sum_{b=|N_s-N_r|}^{(N_s+N_r)a-2a^2} \sum_{k=1}^{\min(N_r,N_d)} \sum_{l=|N_r-N_d|}^{(N_r+N_d)k-2k^2}$, $\Theta_1 = d_1(a,b)d_2(k,l)\phi$, $\Theta_2 = \frac{d_1(a,b)d_2(k,l)}{(c)!}\left(\frac{a}{\bar{\gamma}_1}\right)^c$, $\Theta_3 = \frac{d_1(a,b)d_2(k,l)}{(m)!}\left(\frac{k}{\bar{\gamma}_2}\right)^k$, $\Theta_4 = \frac{d_1(a,b)d_2(k,l)}{(c)!\,(m)!}\left(\frac{a}{\bar{\gamma}_1}\right)^c\left(\frac{k}{\bar{\gamma}_2}\right)^k$ and $\mathcal{I}_n(\mu) = \Gamma(n)\mathrm{e}^{\mu}\sum_{i=1}^{n}\frac{\Gamma(-n+i,\mu)}{\mu^i}$.

3) Truncated channel inversion with fixed rate: The channel capacity under truncated channel inversion with fixed rate is given by $C_{\text{TCIFR}} = \frac{B}{2\ln(2)}\ln\left(1 + \left[\int_{\gamma_0}^{\infty} x^{-1} f_{\gamma_{eq}}(x)\,\mathrm{d}x\right]^{-1}\right)\bar{F}_{\gamma_{eq}^{ub}}(\gamma_0)$, where $\bar{F}_{\gamma_{eq}^{ub}}(\gamma_0)$ is the complementary CDF of γ_{eq}^{ub} evaluated at γ_0. A tight upper bound for C_{TCIFR} can be derived by using the closed-form expressions for $\int_{\gamma_0}^{\infty} x^{-1} f_{\gamma_{eq}^{ub}}(x)\,\mathrm{d}x$ and $\bar{F}_{\gamma_{eq}^{ub}}(\gamma_0)$ given in (53) and (54), respectively.

B. Multiuser relay networks

1) Multiuser relay networks without user scheduling: We consider a multiuser AF relay network having MIMO-enabled single-source, single-relay and L destinations ($D_l|_{l=1}^{L}$)[10]. Both the source and relay are equipped with N_s and N_r antennas whereas the L destinations are single-antenna terminals. This scenario arises in practice, where the base-station communicates with multiple single-antenna mobile terminals with the aid of an infrastructure relay constituting a downlink broadcast channel.

In the first time-slot, S transmits N_s parallel data streams by using transmit precoding matrix $\hat{\mathbf{U}}_1$ and R receives it by using the receiver filtering matrix $\hat{\mathbf{V}}_1$ as[11]

$$\mathbf{Y}_R = \hat{\mathbf{U}}_1^H\left[\sqrt{\mathcal{P}_1}\mathbf{H}_1\hat{\mathbf{V}}_1\mathcal{X} + \mathbf{n}_1\right] = \sqrt{\mathcal{P}_1}\vartheta_l\hat{\mathbf{\Sigma}}_1\mathcal{X} + \hat{\mathbf{n}}_R, \quad (25)$$

where $\hat{\mathbf{n}}_R \sim \mathcal{CN}(0, (\mathcal{P}_1\zeta_1^2 + \sigma_1^2)\mathbf{I}_{N_r})$ is the effective noise vector [22].

In the second time-slot, the relay broadcast $\mathbf{Y}_R$ to L destinations by using transmit zero forcing (ZF) beamforming [31]. The received symbol vector at L destinations is given by

$$\begin{aligned}\mathbf{Y}_D &= \hat{G}_R\mathbf{H}_2\hat{\mathbf{W}}_R\mathbf{\Pi}_R\mathbf{Y}_R + \mathbf{n}_L \\ &= \sqrt{\mathcal{P}_1}\hat{G}_R\vartheta_1\left(\vartheta_2\mathbf{I}_L + \zeta_2\mathbf{E}_2\hat{\mathbf{W}}_R\right)\mathbf{\Pi}\hat{\mathbf{\Sigma}}_1\mathcal{X} \\ &\quad + \hat{G}_R\left(\vartheta_2\mathbf{I}_L + \zeta_2\mathbf{E}_2\hat{\mathbf{W}}_R\right)\mathbf{\Pi}_R\hat{\mathbf{n}}_R + \mathbf{n}_L, \end{aligned} \quad (26)$$

where $\hat{\mathbf{W}}_R$ is the transmit ZF beamformer constructed by taking the pseudo-inverse of $\hat{\mathbf{H}}_2$ as $\hat{\mathbf{W}}_R = \hat{\mathbf{H}}_2^H(\hat{\mathbf{H}}_2\hat{\mathbf{H}}_2^H)^{-1}$ [31]. In (26), $\mathbf{\Pi}_R$ is a $L \times N_r$ permutation matrix[12], which ensures only L data streams pertaining to L destinations are transmitted by the relay. Moreover, $\hat{G}_R$ is the long-term power normalizing factor introduced by R and given by $\hat{G}_R^2 = \sqrt{(\mathcal{P}_2/((\mathcal{P}_1\zeta_1^2 + \sigma_1^2)\mathcal{T}_1 + \mathcal{P}_1\vartheta_2^2\mathcal{T}_2)}$, where $\mathcal{T}_1 = \mathrm{Tr}\{\mathcal{E}\left[\hat{\mathbf{W}}_R\hat{\mathbf{W}}_R^H\right]\} = L/(N_r - L)$ and $\mathcal{T}_2 = \mathrm{Tr}\{\mathcal{E}\left[\hat{\mathbf{W}}_R\hat{\mathbf{\Sigma}}_1\hat{\mathbf{\Sigma}}_1^H\hat{\mathbf{W}}_R^H\right]\}$. In (26), $\mathbf{n}_L$ is the $L \times 1$ Gaussian noise vector with mean zero and variance σ_2^2.

Eq. (26) clearly reveals that the orthogonality of the transmit ZF does not hold due to the imperfect CSI. In this context, the received signal at the l-th destination is given by

$$\begin{aligned} y_{D,l} &= \sqrt{\mathcal{P}_1}\hat{G}_R\vartheta_1 x_l\left(\vartheta_2\sqrt{\hat{\lambda}_1} + \zeta_2\left[\mathbf{E}_2\hat{\mathbf{W}}_R\mathbf{\Pi}\hat{\mathbf{\Sigma}}_1\right]_{l,l}\right) \\ &\quad + \sqrt{\mathcal{P}_1}\hat{G}_R\vartheta_1\zeta_2\sum_{j\neq l,l=1}^{L} x_j\left[\mathbf{E}_2\hat{\mathbf{W}}_R\mathbf{\Pi}\hat{\mathbf{\Sigma}}_1\right]_{j,l} \\ &\quad + \hat{G}_R\left[\left(\vartheta_2\mathbf{I}_L + \zeta_2\mathbf{E}_2\hat{\mathbf{W}}_R\right)\mathbf{\Pi}_R\hat{\mathbf{n}}_R\right]_l + [\mathbf{n}_L]_l. \end{aligned} \quad (27)$$

The first and second terms of (27) account for the desired signal and the inter-user interference, respectively, and the remaining terms represent the effective noise. Thus, the signal-to-interference ratio (SINR) at the l-th destination can be derived as

$$\gamma_{eq}^{(l)} = \frac{\mathcal{P}_1\vartheta_1^2\left|\left(\vartheta_2\sqrt{\hat{\lambda}_1} + \zeta_2\left[\mathbf{E}_2\hat{\mathbf{W}}_R\mathbf{\Pi}\hat{\mathbf{\Sigma}}_1\right]_{l,l}\right)\right|^2}{N+I}, \quad (28)$$

where $N + I$ is given by

$$\begin{aligned} N + I &= \mathcal{P}_1\vartheta_1^2\zeta_2^2\sum_{j\neq l,l=1}^{L}\left|\left[\mathbf{E}_2\hat{\mathbf{W}}_R\mathbf{\Pi}\hat{\mathbf{\Sigma}}_1\right]_{j,l}\right|^2 \\ &\quad + \left(\vartheta_2^2 + \zeta_2^2\left[\mathbf{E}_2\hat{\mathbf{W}}_R\hat{\mathbf{W}}_R^H\mathbf{E}_2^H\right]_{l,l}\right)\left(\mathcal{P}_1\zeta_1^2 + \sigma_1^2\right) + \sigma_2^2/\hat{G}_R^2. \end{aligned} \quad (29)$$

Unfortunately, statistical characterization of (28) appears mathematically intractable. Thus, the ergodic sum capacity of the multi-user MIMO relay network under imperfect CSI

[10] It is assumed that $N_r \geq N_s$ and $N_r > L$.

[11] The beamforming matrices $\hat{\mathbf{U}}_1$ and $\hat{\mathbf{V}}_1$ are formulated by using the imperfect CSI, i.e., $\hat{\mathbf{H}}_1 = \hat{\mathbf{U}}_1\hat{\mathbf{\Sigma}}_1\hat{\mathbf{V}}_1^H$.

[12] The permutation matrix, $\mathbf{\Pi}_i$, can be constructed by horizontally concatenating a $L \times L$ permutation matrix and a $L \times (N_R - L)$ zero matrix.

is investigated by using Monte-Carlo simulations[13]. However, (28) can be simplified under the perfect CSI assumption (i.e., $\vartheta_i = 1$ and $\zeta_i = 0$ for $i \in \{1, 2\}$) to obtain the e2e SNR of the signal received at the l-th destination as

$$\gamma_{eq}^{(l)} = \frac{\bar{\gamma}_1 \lambda_l}{\frac{\mathcal{I}_1}{\bar{\gamma}_2} + \frac{\bar{\gamma}_1 \mathcal{I}_2}{\bar{\gamma}_2} + 1}, \tag{30}$$

where λ_l is the l-th largest eigenvalue of the Wishart matrix $\mathbf{H}_1 \mathbf{H}_1^H$.

In order to highlight the significance of (30), the ergodic sum capacity of a multiuser MIMO relay network with $N_s = 3$, $N_r = 3$ and $L = 2$ is derived as (see Appendix VII for the proof)

$$C = \frac{1}{2\ln(2)} \left[\sum_{n=1}^{5} \frac{\mathbf{a}(n)}{\bar{\gamma}_{eq}} \mathcal{I}_n \left(\bar{\gamma}_{eq}^{-1} \right) - \frac{3}{\bar{\gamma}_{eq}} \mathcal{I}_1 \left(\frac{3}{\bar{\gamma}_{eq}} \right) \right], \tag{31}$$

where $\mathbf{a} = (3, -6, 6, -2, 0.25)$, $\bar{\gamma}_{eq} = \frac{\bar{\gamma}_1}{\frac{\mathcal{I}_1}{\bar{\gamma}_2} + \frac{\bar{\gamma}_1 \mathcal{I}_2}{\bar{\gamma}_2} + 1}$ and $\mathcal{I}_n(\mu) = \Gamma(n) \mathrm{e}^{\mu} \sum_{i=1}^{n} \frac{\Gamma(-n+i, \mu)}{\mu^i}$.

2) Multiuser relay networks with user scheduling: We consider a multiuser AF relay network having beamforming with MIMO-enabled single-source, single-relay and L destinations ($D_l|_{l=1}^{L}$) equipped with N_s, N_r and N_{d_l} antennas, respectively. This network set-up can be seen in practice, where a base-station is communicating with L destinations with the aid of a relay under a multiuser schedule. The SNR optimal scheduling selects the user with the largest e2e SNR. The e2e SNR of the best user is thus given by $\gamma_{eq}^{\mathrm{MRN}} = \frac{\gamma \gamma_{l^*}}{\gamma + \gamma_{l^*} + 1}$, where γ is the $S \to R$ link SNR, and γ_{l^*} is the $R \to D_{l^*}$ link SNR. The best destination D_{l^*} is selected as $l^* = \underset{1 \le l \le L}{\operatorname{argmax}} (\gamma_l)$. This multiuser scheduling algorithm can further be simplified as $l^* = \underset{1 \le l \le L}{\operatorname{argmax}} (\lambda_l)$, where λ_l is the largest eigen value of the channel matrix between the relay and the l-th destination.

Let us consider only the high SNR performance metrics. The asymptotic outage probability and average BER of BPSK can readily be derived by substituting Ω_{MRN} in (32) into (10a) and (11a), respectively.

$$\Omega_{\mathrm{MRN}} = \begin{cases} \frac{\Gamma_n(n)}{\Gamma_n(m+n) k^{N_s N_r}}, & N_s < \sum_{l=1}^{L} N_{d_l} \\ \left(\frac{\Gamma_n(n)}{\Gamma_n(m+n)(k)^{N N_r}} \right. & \\ \left. + \prod_{l=1}^{L} \left[\frac{\Gamma_{n_l}(n_l)}{\Gamma_{n_l}(m_l+n_l) k_l^{N N_l}} \right] \right), & N_s = \sum_{l=1}^{L} N_{d_l} = N \\ \prod_{l=1}^{L} \left[\frac{\Gamma_{n_l}(n_l)}{\Gamma_{n_l}(m_l+n_l) k_l^{N_{d_l} N_r}} \right], & N_s > \sum_{l=1}^{L} N_{d_l} \end{cases} \tag{32}$$

The diversity order of multiuser relay scheduling is given by

$$G_d^{\mathrm{MRN}} = N_r \min \left(N_s, \prod_{l=1}^{L} N_{d_l} \right). \tag{33}$$

C. Best relay selection networks

Consider a MIMO beamforming CA-AF relay network with best relay selection having a single source, Q number of potential relays ($R|_{q=1}^{Q}$), and a single destination, each equipped with N_s, N_{r_q} and N_d antennas, respectively. In best relay selection, the R_{q^*}-th relay is selected as $q^* = \underset{1 \le q \le Q}{\operatorname{argmax}} \left(\frac{\gamma_{s,R_q} \gamma_{R_q D}}{\gamma_{s,R_q} + \gamma_{R_q,D} + 1} \right)$, where γ_{s,R_q} and $\gamma_{R_q,D}$ are $S \to R_q$ and $R_q \to D$ channel SNRs. The asymptotic outage probability can be derived as

$$P_{\mathrm{out}}^{\infty} = \left(\prod_{q=1}^{Q} \Omega_q \right) \left(\frac{\gamma_{th}}{\bar{\gamma}} \right)^{\sum_{q=1}^{Q} G_{d_l}} + o\left(\bar{\gamma}^{-(\sum_{q=1}^{Q} G_{d_l} + 1)} \right), \tag{34}$$

where Ω_q can be obtained by replacing N_r of Ω in (10a) by N_{r_q}, and $G_{d_l} = N_{r_q} \min(N_s, N_d)$. Similarly, the asymptotic BER of BPSK is given by

$$\bar{P}_e^{\infty} = \frac{\left(\prod_{q=1}^{Q} \Omega_q \right) \Gamma(G_d^{\mathrm{BRS}} + \frac{1}{2})}{2\sqrt{\pi} (\bar{\gamma})^{G_d^{\mathrm{BRS}}}} + o\left(\bar{\gamma}^{-(G_d^{\mathrm{BRS}} + 1)} \right), \tag{35}$$

where the diversity order is $G_d^{\mathrm{BRS}} = \min(N_s, N_d) \sum_{q=1}^{Q} N_{r_q}$.

D. Multi-hop MIMO AF relay networks

Consider a L-hop ($L \ge 2$) MIMO beamforming relay network having $L+1$ terminals each equipped with $N_l|_{l=1}^{L+1}$ antennas. The asymptotic outage probability can be derived as follows:

$$P_{\mathrm{out,MH}}^{\infty} = \sum_{l} \frac{\Theta_l}{G_{d_l} k_l^{G_{d_l}}} \left(\frac{\gamma_{th}}{\bar{\gamma}} \right)^{G_d^{\mathrm{MH}}} + o\left(\bar{\gamma}^{-(G_d^{\mathrm{MH}} + 1)} \right), \tag{36}$$

where $l \in \{ l | G_{d_l} = \min_{1 \le l \le L} (N_l N_{l+1}), 1 \le l \le L \}$, $k_l = \bar{\gamma}_l / \bar{\gamma}$, and $G_d^{\mathrm{MH}} = \min_{1 \le l \le L} (G_{d_l})$. Here, G_{d_l} is the diversity order of the l-th hop; $G_{d_l} = N_l N_{l+1}$. Here, $\Theta_l = \frac{(N_l N_{l+1}) \Gamma_{U_l}(U_l)}{\Gamma_{U_l}(U_l + V_l)}$, where $U_l = \min(N_l, N_{l+1})$, $V_l = \max(N_l, N_{l+1})$. Similarly, the asymptotic BER of BPSK can be derived as

$$\bar{P}_{\mathrm{e,MH}}^{\infty} = \frac{\Gamma\left(G_d^{\mathrm{MH}} + \frac{1}{2}\right)}{2\sqrt{\pi} G_d^{\mathrm{MH}} (\bar{\gamma})^{G_d^{\mathrm{MH}}}} \sum_{l} \frac{\Theta_l}{(k_l)^{G_{d_l}}} + o\left(\bar{\gamma}^{-(G_d^{\mathrm{MH}} + 1)} \right). \tag{37}$$

By using (37), the diversity order and the array gain can be obtained as

$$G_d^{\mathrm{MH}} = \min_{1 \le l \le L} (N_l N_{l+1}) \text{ and } G_a^{\mathrm{MH}} = \left[\frac{\Gamma\left(G_d^{\mathrm{MH}} + \frac{1}{2}\right)}{2\sqrt{\pi} G_d^{\mathrm{MH}}} \sum_{l} \frac{\Theta_l}{k_l^{G_{d_l}}} \right]^{\frac{-1}{G_d^{\mathrm{MH}}}}. \tag{38}$$

The overall diversity order is thus governed by the hops having the lowest diversity orders.

V. Numerical Results

This section presents the numerical results and verifies our analysis through Monte-Carlo simulations. To capture the effect of the network geometry, the average SNR of the i-th hop is modeled by $\bar{\gamma}_i = \bar{\gamma} (L_0 / L_i)^{\varpi}$, for $l \in \{1, 2\}$, where $\bar{\gamma}$ is the average transmit SNR, L_0 is the reference distance, and ϖ is the path-loss exponent. The distances between the terminals $S \to R$, and $R \to D$ are denoted by L_1 and L_2, respectively.

1) Impact of feedback delays and channel estimation errors on the outage probability: In Fig. 2, the exact outage probability is plotted for $N_s = 3$, $N_r = 2$ and $N_d = 3$ antenna set-up. The exact and asymptotic outage curves for the perfect CSI ($\rho_l = 1$ and $\sigma_{e,l}^2 = 0$) are plotted as a benchmark. Specifically, in Fig. 2, the impact of both the

[13]It is worth noticing that even for single-hop MIMO transmit ZF beamforming systems, the exact analysis under imperfect CSI appears to be mathematically intractable [31].

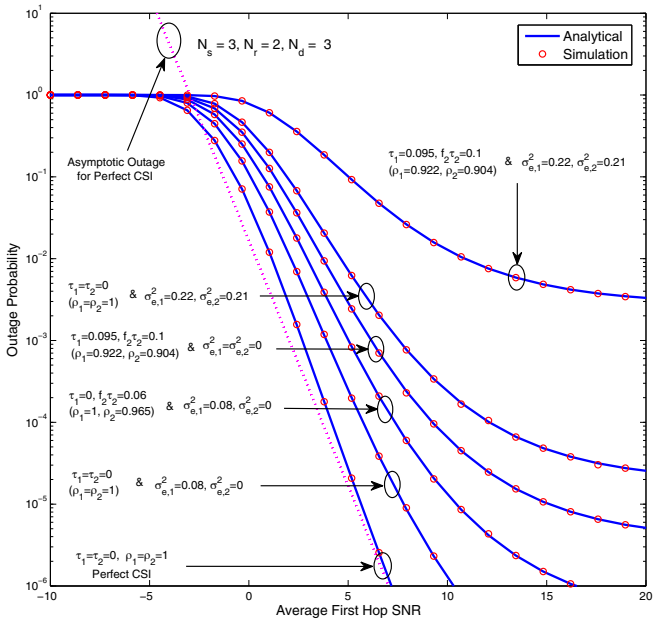

Fig. 2. The impact of outdated CSI and channel estimation errors on the outage probability of MIMO beamforming AF relay networks. The hop distances are $L_1 = 2L_2$ and the path-loss exponent is $\varpi = 2.5$.

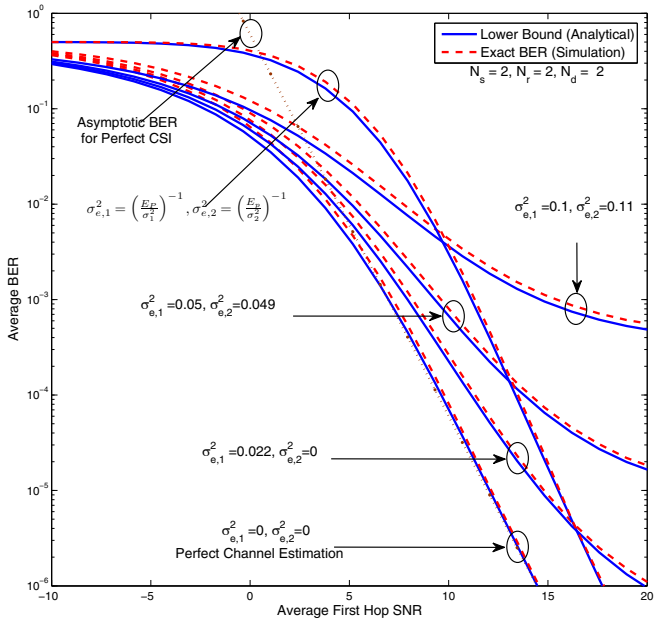

Fig. 3. The impact of channel estimation errors on the average BER of BPSK of MIMO beamforming AF relay networks. The hop distances are $L_1 = 0.75L_2$ and the path-loss exponent is $\varpi = 2.5$.

outdated CSI due to feedback delays and channel estimation errors on the outage probability is shown. The beamforming vectors at S, R and D are selected based on the outdated CSI received via the local feedback channels $R \to S$ and $D \to R$ with time delays τ_1 and τ_2. Moreover, as per (1), the channel estimates are perturbed by Gaussian errors with variances $\sigma^2_{e,1}$ and $\sigma^2_{e,2}$. The analysis and simulations are obtained by using the channel model given in (1). Several outage curves are obtained by changing ρ_1 and ρ_2, where they are related to the time delays by following Clarke's fading model[14]. The outage performance degrades significantly even when the feedback channels and channel estimates experience slight time delays or/and channel estimation errors, respectively. In fact, the achievable diversity gain diminishes completely as the time delay and/or the channel estimation error variance increase in either the $R \to S$ or $D \to R$ feedback channel. The Monte-Carlo simulation points verify that our analysis is accurate.

2) Impact of channel estimation errors on the average BER: In Fig. 3, the BER of BPSK is plotted for $N_s = 3$, $N_r = 2$ and $N_d = 3$ antenna set-up. The BER curve of the perfect CSI ($\sigma^2_{e,l} = 0$) is plotted as a benchmark. In particular, the asymptotic BER shows that the system achieves the full diversity order ($G_d = 4$), and thus verifying our diversity analysis. Specifically, Fig. 3 depicts the effect of channel estimation errors on the BER of BPSK. The channels $S \to R$ and $R \to D$ are modeled by using (1). Even a slight estimation error in either channel degrades the BER performance significantly. When the estimation error is assumed to be fixed, the BER curves exhibit error floors as the average first hop SNR increases. However, in practice, the estimation errors are inversely propositional to the pilot symbol SNR, $\sigma^2_{e,l} \propto \left(E_p/\sigma^2_l\right)$, for $l \in \{1, 2\}$, where E_p is the pilot symbol energy, and σ^2_l is the noise variance [22]. Specifically, when the estimation-error variance decreases as the SNR of the data symbols increases (the pilot symbols have the same energy as the data symbols), the error floors do not occur and the achievable diversity order is likely to be persevered; however, the array gain is severely degraded. As observed with the outage probability, the relays having the knowledge of $\sigma^2_{e,l}$ and ρ_l outperform the relays having no access to $\sigma^2_{e,l}$ and ρ_l in terms of the average BER. The tightness between the analytical lower bounds and the exact Monte-Carlo simulations demonstrates the accuracy of our analysis.

3) Impact of both channel estimation errors and outdated CSI on the average BER: In Fig. 4, the effect of both outdated CSI and channel estimation errors is shown by using the channel model (1). Fig. 4 clearly reveals that their combined effect degrades the system performance more than their individual effects. Monte-Carlo simulations demonstrate the accuracy of the channel model in (1), as well as our analysis.

4) Impact of correlated fading on the outage probability: Fig. 5 shows the effect of correlated fading among the antennas at S, R and D on the outage probability. The transmit and receive arbitrary correlation matrices Υ_1, Υ_2, Ψ_1 and Ψ_2 for uniform linear antenna arrays at S, R and D are constructed by using [32, Eq. (4)]. The amount of spatial correlation between adjacent antenna elements can thus be quantified by using their relative antenna spacing (l_1, l_2), angular spreads $(\sigma^2_{as,1}, \sigma^2_{as,2})$, and the angle of arrival or departure (θ_1, θ_2). Three different correlation scenarios are obtained as (a) high

[14]For Clarke's model, $\rho_1 = \mathcal{J}_0(2\pi f_1 \tau_1)$ and $\rho_2 = \mathcal{J}_0(2\pi f_2 \tau_2)$, where f_1 and f_2 are the Doppler frequencies, and τ_1 and τ_2 are the feedback delays.

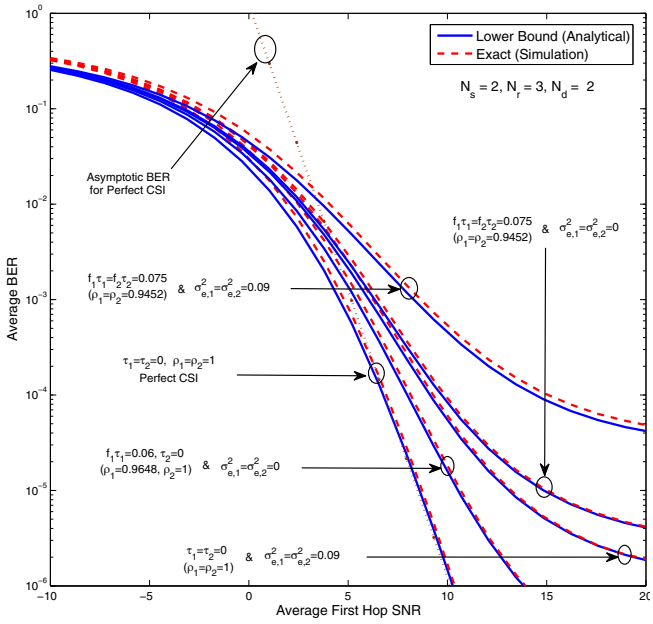

Fig. 4. The impact of both outdated CSI and the channel estimation errors on the average BER of BPSK of MIMO beamforming AF relay networks. The hop distances are $L_1 = L_2$ and the path-loss exponent is $\varpi = 2.5$.

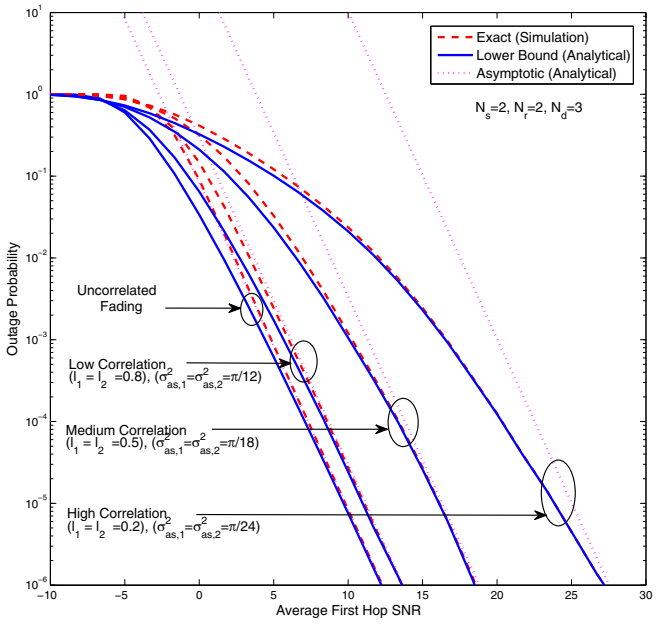

Fig. 5. The impact of spatial correlation on the outage probability of MIMO beamforming AF relay networks. The hop distances are $L_1 = L_2$, and the path-loss exponent is $\varpi = 2.5$.

correlation: $(l_1 = l_2 = 0.2, \sigma^2_{as,1} = \sigma^2_{as,2} = \pi/24)$, (b) medium correlation: $(l_1 = l_2 = 0.5, \sigma^2_1 = \sigma^2_2 = \pi/18)$, and (c) low correlation: $(l_1 = l_2 = 0.8, \sigma^2_{as,1} = \sigma^2_{as,2} = \pi/12)$. Since l_1 and l_2 are the relative antenna spacing, and $\sigma^2_{as,1}$ and $\sigma^2_{as,2}$ are the angular spreads, smaller values of l_1, l_2, $\sigma^2_{as,1}$ and $\sigma^2_{as,2}$ result

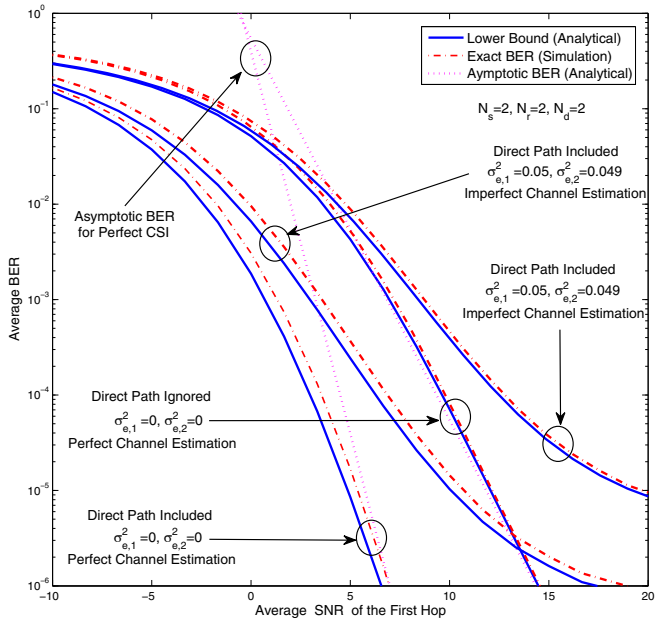

Fig. 6. The impact of direct channel on the average BER of BPSK of MIMO beamforming AF relay networks. The hop distances are $L_1 = L_2$, and the path-loss exponent is $\varpi = 2.5$.

in higher spatial correlation [32]. The higher correlation effects at S, R and D degrade the outage performance significantly. In fact, at 10^{-5} outage probability, a 14 dB loss is incurred when the high correlation fading in effect over the uncorrelated fading. The asymptotic BER curves reveal that the amount of correlation does not affect the achievable diversity order, but the array gain is severely affected by higher correlation. Our outage lower bounds are not only tight in the moderate-to-high SNR regime but also asymptotically exact at high SNRs, and hence, may render then useful in practical system designs. The exact outage curves are plotted by using Monte-Carlo simulations.

5) Impact of the direct channel: In Fig. 6, the effect of the presence of a direct channel between S and D on the average BER of BPSK is studied. In particular, two sets of BER curves, (i) direct channel is included, and (ii) direct channel is ignored, are plotted for comparison purposes. The asymptotic BER curves in Fig. 6 clearly reveal that the presence of a direct channel improves the achievable diversity order considerably. For example, at 10^{-5} BER, the system with direct channel provides a 8 dB relative gain over the system without direct channel. Moreover, the adverse effect of channel estimation errors on the BER is shown. Specifically, the exact BER curves are plotted by using (16), which has already been reported in [12]. Further, the lower bound, which is plotted by using (21), is significantly tight in low-to-high SNR regime to the exact BER in (16), and hence, verifies our bounding technique given in (18) and its computational accuracy.

6) Capacity bounds for adaptive transmission: Fig. 7 shows the performance of adaptive transmission for MIMO beamforming AF relay networks in terms of channel capacity. The exact capacity curves are plotted by using Monte-Carlo

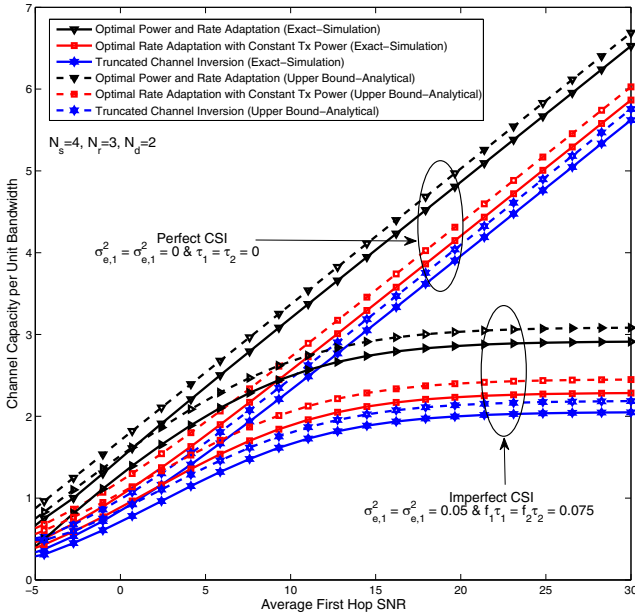

Fig. 7. The capacity bounds of MIMO beamforming AF relay networks with adaptive transmission. The hop distances are $L_1 = L_2$ and the path-loss exponent is $\varpi = 2.5$.

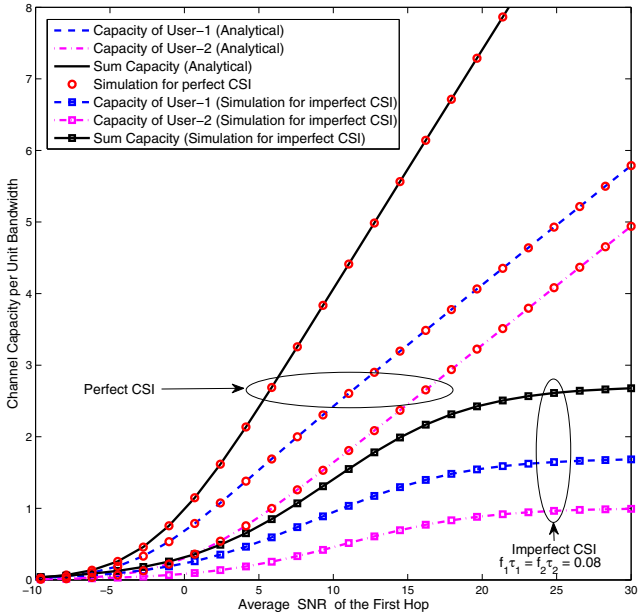

Fig. 8. The sum capacity of multiuser relay networks without user scheduling. The source and relay are equipped with $N_s = 3$, and $N_r = 3$ antennas. Two single-antenna destinations are considered. The hop distances are $L_1 = 2L_2$ and the path-loss exponent is $\varpi = 2.5$.

simulations whereas the upper bounds are plotted by using (23), (24) and (53). The optimal power and rate adaptation provides the highest capacity gain whereas the truncated channel inversion performs the worst in comparison with the optimal rate adaptation with fixed transmit power. Fig. 7 also reveals that the presence of feedback delays and channel estimation errors causes severe detrimental impact on the capacity bounds. Our capacity upper bounds are relatively tight in the entire SNR regime and can be used to obtain valuable system-design insights.

7) Sum capacity of Multiuser relay networks (MRN) without user scheduling: In Fig. 8, both the sum capacity and the individual capacity of MRN without user scheduling is plotted. The system set-up consists of a source and a relay, both equipped with three antennas, and two single antenna destinations. Since the individual e2e SNR is solely governed by the ordered singular values of the first hop channel matrix, the individual capacity of destinations vary accordingly. Fig. 8 clearly reveals that our system set-up provides significant gains in terms of the ergodic sum capacity under the perfect CSI. Counter intuitively, imperfect CSI due to feedback delays has a severe detrimental impact on the system capacity. This observation is not surprising as the imperfect CSI for transmit ZF beamforming results in inter-user interference.

8) MRN with user scheduling, best relay selection (BRS) networks and multi-hop relay networks: Fig. 9 shows the BPSK average BER of two network scenarios: (i) MRN and (ii) BRS network. The exact BER curves are plotted by using Monte-Carlo simulation results, and the asymptotic BER curves are plotted by using the results in Sections IV-B and IV-C. Two MRN set-ups are considered, (i) $N_s = 2, N_r = 1$ and $N_{d_l} = 2$ for $l \in \{1, 2, 3\}$, and (ii) $N_s = 2, N_r = 2$ and $N_{d_l} = 2$ for $l \in \{1, 2, 3\}$. Similarly, two BRS network set-ups are also considered: (i) $N_s = 2, N_d = 2$ and $N_{r_q} = 1$ for $q \in \{1, 2, 3\}$, and (ii) $N_s = 2, N_d = 2$ and $N_{r_q} = 2$ for $q \in \{1, 2, 3\}$. In both the MRN and the BRS cases, the corresponding set-up (ii) always outperforms the set-up (i) because of set-up (ii)'s higher number of antennas at the relay terminals. In Fig. 10, the exact and asymptotic BER curves of four-hop MIMO beamforming relaying are plotted to verify our analysis in Section IV-D. Our asymptotic BER curves accurately reveal the diversity order and array gains of all three systems.

VI. Conclusion

The performance of dual-hop MIMO AF relay networks with hop-by-hop beamforming was studied. To this end, the outage probability, average BER and ergodic capacity were derived. The performance impact of spatially-correlated fading, outdated CSI and channel estimation errors was derived, thereby quantifying the amount of performance degradation. Our results show that these practical transmission impairments result in significant performance degradations. As well, the impact of a presence of the direct channel between the source and the destination was studied, and the resulting performance improvement was quantified. Specifically, valuable system-design parameters such as the diversity order and array gains were derived by using our asymptotic analysis of performance metrics. Furthermore, four applications of our main results; (i) adaptive transmission with beamforming, (ii) multiuser relay networks, (iii) best relay selection networks, and (iv) multi-hop relay networks were presented to illustrate the usefulness and applicability. The analytical results were validated through Monte-Carlo simulations. Our analytical and simulation results

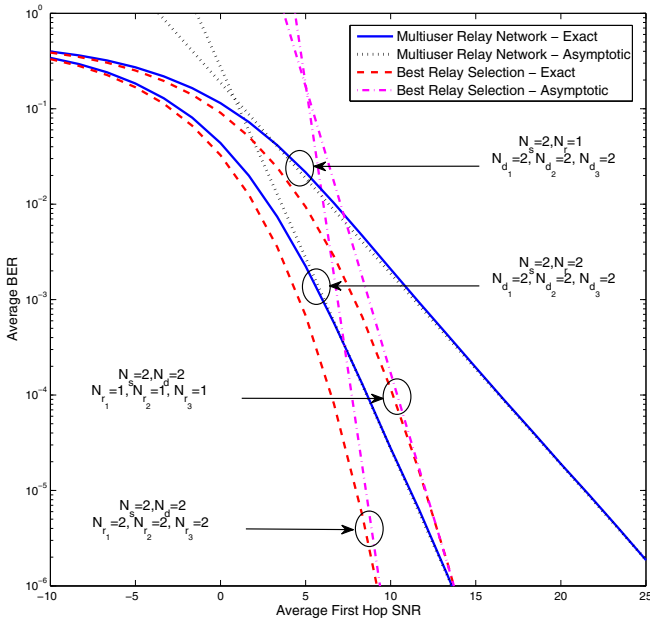

Fig. 9. The average BER of BPSK for multiuser relay networks and best relay selection networks with MIMO beamforming AF relay networks. The hop distances are $L_1 = 2L_2$ and the path-loss exponent is $\varpi = 2.5$.

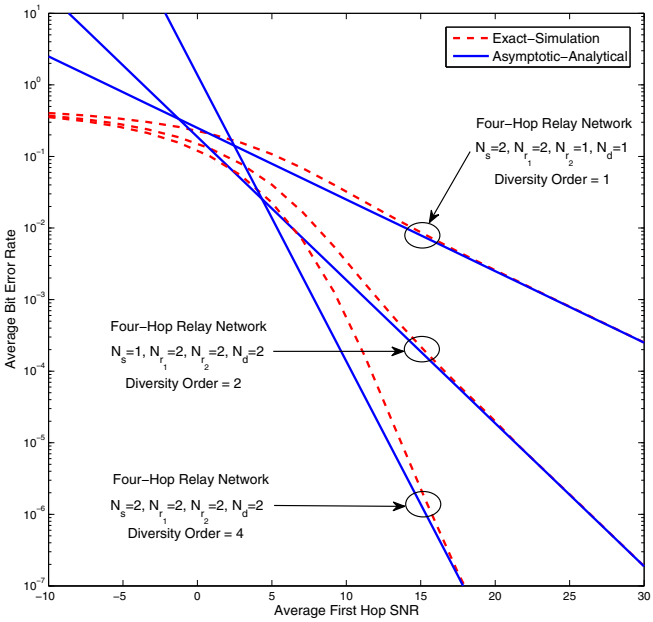

Fig. 10. The average BER of BPSK for a four-hop MIMO beamforming AF relay network. The hop distances are $L = [0.25L_0, 0.15L_0, 0.20L_0, 0.40L_0]$ and the path-loss exponent is $\varpi = 2.5$.

provide valuable insights for designing practical dual-hop MIMO relay networks with beamforming.

Appendix I
Proof of the CDF of End-to-End SNR

The CDF of γ_{eq} in (5b) can be derived as follows: $F_{\gamma_{eq}}(x) = \Pr(\gamma_1\gamma_2/(\alpha\gamma_1+\gamma_2+\beta) \le x) = F_{\gamma_1}(x) + \int_x^\infty \Pr(\gamma_2 \le (\alpha y+\beta)x/(y-x))\, f_{\gamma_1}(y)\,\mathrm{d}y$. By using a variable change $z = y - x$, $F_{\gamma_{eq}}(x)$ can be expressed in a compact form as $F_{\gamma_{eq}}(x) = 1 - \int_0^\infty \bar{F}_{\gamma_2}([\alpha(x+z)+\beta]x/z) f_{\gamma_1}(z+x)\mathrm{d}z$, where $f_{\gamma_1}(x)$ is the PDF of γ_1 and $\bar{F}_{\gamma_2}(x)$ is the complementary cumulative distribution function (CCDF) of γ_2. In order to derive $F_{\gamma_{eq}}(x)$, one needs the closed-form statistics of $\hat{\lambda}_1$ and $\hat{\lambda}_2$, the largest eigenvalues of the central Wishart matrices, $\hat{\mathbf{H}}_1\hat{\mathbf{H}}_1^H$ and $\hat{\mathbf{H}}_2\hat{\mathbf{H}}_2^H$, respectively. By using [3], [22], $f_{\gamma_1}(x)$ can be obtained as

$$f_{\gamma_1}(x) = \sum_{a=1}^{\min(N_s,N_r)} \sum_{b=|N_s-N_r|}^{(N_s+N_r)a-2a^2} \frac{a^{b+1} d_1(a,b)}{(\bar{\gamma}_1)^{b+1}\,(b)!} x^b \mathrm{e}^{-\frac{ax}{\bar{\gamma}_1}}. \quad (39)$$

Similarly, $\bar{F}_{\gamma_2}(x)$ can readily be derived as

$$\bar{F}_{\gamma_2}(x) = \sum_{k=1}^{\min(N_r,N_d)} \sum_{l=|N_r-N_d|}^{(N_r+N_d)k-2k^2} \sum_{m=0}^{l} \frac{k^m d_2(k,l)}{(\bar{\gamma}_2)^m\,(m)!} x^m \mathrm{e}^{-\frac{kx}{\bar{\gamma}_2}}, \quad (40)$$

where $d_1(a,b)$ and $d_2(k,l)$ are defined in (6). By substituting (39) and (40) into the integral representation of $F_{\gamma_{eq}}(x)$ and evaluating it using [17, Eq. (3.471.9)], the desired result (6) can be derived.

Appendix II
Proof of the MGF of End-to-End SNR

The MFG of the e2e SNR can be derived as follows:

$$\mathcal{M}_{\gamma_{eq}}(s) = \int_0^\infty \mathrm{e}^{-sx} f_{\gamma_{eq}}(x)\,\mathrm{d}x = 1 - \int_0^\infty s\mathrm{e}^{-sx}\big[1 - F_{\gamma_{eq}}(x)\big]\mathrm{d}x. \quad (41)$$

However, the integral resulting by substituting (6) into (41) does not render itself to a closed-form solution. Hence an upper bound of the e2e SNR, which lends itself to analytic MGF expression is formulated as [33]

$$\gamma_{eq} = \frac{\gamma_1\gamma_2}{\alpha\gamma_1+\gamma_2+\beta} \le \frac{\gamma_1\gamma_2}{\alpha\gamma_1+\gamma_2} = \gamma_{eq}^{ub}. \quad (42)$$

Specifically, γ_{eq}^{ub} in (42) provides asymptotically exact and tight SNR bound for γ_{eq} in moderate-to-high SNR regime [26], [33]. Now by substituting (6) with $\beta = 0$ into (41), a single-integral expression is obtained as

$$\mathcal{M}_{\gamma_{eq}^{ub}}(s) = 1 - \sum_{a,b,k,l,m} \sum_{u=0}^{m+b} \frac{2\binom{m+b}{u} d_1(a,b) d_2(k,l)}{b!\; m! (a)^{\frac{u-m-2b-1}{2}}} \times \frac{(\alpha k)^{\frac{u+m+1}{2}}}{(\bar{\gamma}_1)^{\frac{2b-u+m+1}{2}} (\bar{\gamma}_2)^{\frac{u+m+1}{2}}} \mathbb{J}_{\mu,\nu,\psi,\omega}(s), \quad (43a)$$

where the integral $\mathbb{J}_{\mu,\nu,\psi,\omega}(s)$ is given by

$$\mathbb{J}_{\mu,\nu,\psi,\omega}(s) = \int_0^\infty s x^{m+b+1} \mathrm{e}^{-x\left(s+\frac{a}{\bar{\gamma}_1}+\frac{k}{\bar{\gamma}_2}\right)} \mathcal{K}_{u-m+2}\left(2x\sqrt{\frac{ka\alpha}{\bar{\gamma}_1\bar{\gamma}_2}}\right)\mathrm{d}x. \quad (43b)$$

In (43b), μ, ν, ψ, and ω are defined as $\mu = m+b+2$, $\nu = u-m+1$, $\psi = s + \frac{a}{\bar{\gamma}_1} + \frac{\alpha k}{\bar{\gamma}_2}$, and $\omega = 2\sqrt{ka\alpha/(\bar{\gamma}_1\bar{\gamma}_2)}$, respectively. Now, $\mathbb{J}_{\mu,\nu,\psi,\omega}(s)$ can be solved by using [17, Eq. (6.621.3)] as in (7a).

APPENDIX III
PROOF OF THE BER OF BPSK

The average BER, $\bar{P}_e$, can be derived by averaging the conditional BER over the SNR PDF as $\bar{P}_e = \int_0^\infty \mathcal{Q}\big(\sqrt{2\gamma}\big)\, f_{\gamma_{eq}}(\gamma)\,\mathrm{d}\gamma$. Alternatively, $\bar{P}_e$ can also be written as $\bar{P}_e = 1/2 - 1/2\sqrt{1/\pi}\int_0^\infty \gamma^{-\frac{1}{2}}\mathrm{e}^{-\gamma}\big[1-F_{\gamma_{eq}}(\gamma)\big]\,\mathrm{d}\gamma$. A tight and asymptotically exact lower bound of the average BER of BPSK can be derived by substituting (6) with $\beta = 0$ into the integral representation of $\bar{P}_e$ as follows[15] :

$$\bar{P}_e^{lb} = \frac{1}{2} - \frac{1}{2}\sqrt{\frac{1}{\pi}} \sum_{a,b,k,l,m} \sum_{u=0}^{m+b} \frac{2\binom{m+b}{u} d_1(a,b) d_2(k,l)}{b!\; m! (a)^{\frac{u-m-2b-1}{2}}} \times \frac{(\alpha k)^{\frac{u+m+1}{2}}}{(\bar{\gamma}_1)^{\frac{2b-u+m+1}{2}} (\bar{\gamma}_2)^{\frac{u+m+1}{2}}} \mathbb{I}(\mu,\nu,\psi,\omega), \tag{44a}$$

where the integral function $\mathbb{I}(\mu,\nu,\psi,\omega)$ is given by

$$\mathbb{I}(\mu,\nu,\psi,\omega) = \int_0^\infty x^{m+b+\frac{1}{2}} \mathrm{e}^{-x\left(1+\frac{a}{\bar{\gamma}_1}+\frac{k}{\bar{\gamma}_2}\right)} \mathcal{K}_{u-m+1}\left(2x\sqrt{\frac{ka\alpha}{\bar{\gamma}_1\bar{\gamma}_2}}\right)\mathrm{d}x. \tag{44b}$$

In (44a), μ, ν, ψ, and ω are defined as $\mu = m + b + \frac{3}{2}$, $\nu = u - m + 1$, $\psi = 1 + \frac{a}{\bar{\gamma}_1} + \frac{\alpha k}{\bar{\gamma}_2}$, and $\omega = 2\sqrt{ka\alpha/(\bar{\gamma}_1\bar{\gamma}_2)}$, respectively. The integral (44a) can be evaluated by using [17, Eq. (6.621.3)] as given in (9a).

APPENDIX IV
A UNIFIED HIGH SNR ANALYSIS FOR HOP-BY-HOP MIMO TRANSMISSION SCHEMES

This section provides a unified high SNR analysis for multi-hop ($L \geq 1$) MIMO CA-AF relay networks with hop-by-hop transmission schemes, for example, beamforming, TAS/MRC, and transmit/receive antenna selection, etc., or any combination of these schemes. For such schemes, the l-th hop SNR can always be independently decomposed and its CDF an PDF can be approximated by a single term polynomial approximation, which is exact at high average transmit SNR $\bar{\gamma}$, as

$$F_{\gamma_l^\infty}(x) = \frac{\beta_l x^{d_l}}{d_l\,(\bar{\gamma}_l)^{d_l}} + o\big(x^{d_l+1}\big)\,,\; f_{\gamma_l^\infty}(x) = \frac{\beta_l x^{d_l-1}}{(\bar{\gamma}_l)^{d_l}} + o\big(x^{d_l}\big), \tag{45}$$

where the l-th hop average SNR is given by $\bar{\gamma}_l = k_l\bar{\gamma}$. Let us start with the asymptotically exact multi-hop SNR upper bound in [26], $\gamma_{eq} = \left[\sum_{l=1}^L \frac{1}{\gamma_l}\right]^{-1} \leq \gamma_{eq}^{\text{ub}} = \left(\frac{1}{X_1} + \frac{1}{X_2}\right)^{-1}$, where $X_1 = \min_{1\leq l\leq P}(\gamma_l)$ and $X_2 = \min_{P+1\leq l\leq L}(\gamma_l)$. The asymptotic CDFs of X_1 can be derived by using substituting (45) into $F_{X_1}(x) = 1 - \prod_{l=1}^P (1 - F_{\gamma_l}(x))$ and by using the identity, $\prod_{l=1}^L (1 - x_l) = 1 + \sum_{l=1}^L (-1)^l \sum_{\lambda_1=1}^{L-l+1} \sum_{\lambda_2=\lambda_1+1}^{L-l+2} \cdots\cdots \sum_{\lambda_l=\lambda_{l-1}}^{L} \prod_{n=1}^l x_{\lambda_n}$, as follows:

$$F_{X_1^\infty}(x) = \sum_l \frac{\beta_l}{d_l k_l^{d_l}} \left(\frac{x}{\bar{\gamma}}\right)^{d_1^{\min}} + o\Big(x^{d_1^{\min}+1}\Big), \tag{46}$$

[15]It is assumed that an exact phase reference can be maintained with respect to the signal component in the destination receiver, which is reasonable for slow fading channels.

where $l \in \{l | d_l = d_1^{\min}, 1 \leq l \leq P\}$ and $d_1^{\min} = \min_{1\leq l\leq P}(d_l)$. Similarly, the asymptotic CDF of X_2 can be derived as

$$F_{X_2^\infty}(x) = \sum_l \frac{\beta_l}{d_l k_l^{d_l}} \left(\frac{x}{\bar{\gamma}}\right)^{d_2^{\min}} + o\Big(x^{d_2^{\min}+1}\Big), \tag{47}$$

where $l \in \{l | d_l = d_1^{\min}, P+1 \leq l \leq L\}$ and $d_2^{\min} = \min_{P+1\leq l\leq L}(d_l)$. The CDF of γ_{eq}^{ub} can then be derived as [4]

$$F_{\gamma_{eq}^{\text{ub}}}(x) = \Pr\left(\frac{X_1X_2}{X_1+X_2} \leq x\right) = \int_0^x \underbrace{\Pr\left(X_1 \geq \frac{\lambda x}{\lambda - x}\right)}_{=1} f_{X_2}(\lambda)\mathrm{d}\lambda + \int_x^\infty \Pr\left(X_1 \leq \frac{\lambda x}{\lambda - x}\right) f_{X_2}(\lambda)\mathrm{d}\lambda. \tag{48}$$

If $x \to 0^+$, then $\lambda x/(\lambda - x) \to 0^+$. Thus, without loss of generality, $F_{\gamma_{eq}^{\text{ub}}}(x)$ can further be simplified by using the asymptotically exactness of γ_{eq}^{ub} to γ_{eq} as $F_{\gamma_{eq}^\infty}(x) = F_{X_1^\infty}(x) + \lim_{x\to 0^+} \Pr(X_1 \leq x) \int_x^\infty f_{X_2}(\lambda)\mathrm{d}\lambda = F_{X_1^\infty}(x) + F_{X_2^\infty}(x) - F_{X_1^\infty}(x)\, F_{X_2^\infty}(x)$. For beamforming, β_l in (45) is given by [34] $\beta_l = (N_l N_{l+1})\Gamma_{U_l}(U_l)/\Gamma_{U_l}(U_l+V_l)$, where N_l and N_{l+1} are the number of antennas at the l-th hop transmitter and receiver, and the desired results can be derived as in (10a) and (36).

APPENDIX V
HIGH SNR BER APPROXIMATION WITH THE DIRECT CHANNEL

The single term polynomial CDF approximation for $x \to 0^+$ of the direct channel SNR can readily be obtained by using (19) and [34] as follows:

$$F_{\gamma_{\text{SD}}^\infty}(x) = \frac{\Gamma_{n_0}(n_0)}{\Gamma_{n_0}(m_0+n_0)k_0^{N_sN_d}} \left(\frac{x}{\bar{\gamma}}\right)^{N_s+N_d} + o\Big(x^{-(N_sN_d+1)}\Big). \tag{49}$$

The corresponding single term polynomial CDF approximation for $x \to 0^+$ of the relayed-channel SNR has already been derived in Section III-D and can be obtained by replacing γ_{th} in (10a) by x. Next, the single term polynomial approximation of the effective e2e SNR by considering both the direct channel and the relayed-channel can be derived as follows:

For the sake of notational simplicity, the single term polynomial CDF approximations for $x \to 0^+$ of the relayed-channel and direct channel SNRs are denoted by $F_{\gamma_{\text{SRD}}^\infty}(x) = \Omega_{\text{SRD}}\,(x/\bar{\gamma})^{G_{d_{\text{SRD}}}} + o\Big(x^{-(G_{d_{\text{SRD}}}+1)}\Big)$, and $F_{\gamma_{\text{SD}}^\infty}(x) = \Omega_{\text{SD}}\,(x/\bar{\gamma})^{G_{d_{\text{SD}}}} + o\big(x^{-(G_{d_{\text{SD}}}+1)}\big)$, respectively. The single term polynomial approximations for the MGFs of γ_{SRD} and γ_{SD} can be derived by substituting $F_{\gamma_{\text{SRD}}^\infty}(x)$ and $F_{\gamma_{\text{SD}}^\infty}(x)$ into $\mathcal{M}_\Lambda(s) = \int_0^\infty sF_\Lambda(x)\,\mathrm{e}^{-sx}\mathrm{d}x$ as follows [35]: $\mathcal{M}_{\gamma_{\text{SRD}}^\infty}(s) = \Omega_{\text{SRD}}\Gamma(G_{d_{\text{SRD}}}+1)/(\bar{\gamma}s)^{G_{d_{\text{SRD}}}} + o\left(s^{-(G_{d_{\text{SRD}}}+1)}\right)$ and $\mathcal{M}_{\gamma_{\text{SD}}^\infty}(s) = \Omega_{\text{SD}}\Gamma(G_{d_{\text{SD}}}+1)/(\bar{\gamma}s)^{G_{d_{\text{SD}}}} + o\left(s^{-(G_{d_{\text{SD}}}+1)}\right)$. Next, a single term polynomial approximation of the CDF of the e2e SNR approximation ($\gamma_{\text{eq}}^{\text{approx}} = \gamma_{\text{SD}} + \gamma_{\text{SRD}}$) for $x \to 0^+$ can be derived by using $\mathcal{L}^{-1}\left(\mathcal{M}_{\gamma_{\text{SD}}^\infty}(s)\,\mathcal{M}_{\gamma_{\text{SRD}}^\infty}(s)\,/s\right)$, where $\mathcal{L}^{-1}(\cdot)$ denotes the inverse Laplace transform, as follows:

$$F_{\gamma_{\text{eq}}^{\text{approx},\infty}}(x) = \frac{\Omega_{\text{SD}}\Omega_{\text{SRD}}\Gamma(G_{d_{\text{SD}}}+1)\Gamma(G_{d_{\text{SRD}}}+1)}{\Gamma(G_{d_{\text{SD}}}+G_{d_{\text{SRD}}}+1)} \left(\frac{x}{\bar{\gamma}}\right)^{G_{d_{\text{SD}}}+G_{d_{\text{SRD}}}}$$

$$+ o\left(x^{-(G_{d_{\text{SD}}}+G_{d_{\text{SRD}}}+1)}\right). \quad (50)$$

Next, the asymptotic approximation for the average BER of BPSK at high SNRs can be derived by substituting (50) into $\bar{P}_e^{\infty} = 1/2\sqrt{1/\pi}\int_0^{\infty} x^{-\frac{1}{2}}\mathrm{e}^{-x}F_{\gamma_{eq}^{\text{approx},\infty}}(x)\,\mathrm{d}x$ and evaluating the simple integral by using [17, Eqn. (3.351.3)] as

$$\bar{P}_e^{\infty} = \frac{\Omega_{\text{SD}}\Omega_{\text{SRD}}\Gamma(G_{d_{\text{SD}}}+1)\Gamma(G_{d_{\text{SRD}}}+1)\Gamma(G_{d_{\text{SD}}}+G_{d_{\text{SRD}}}+\frac{1}{2})}{2\sqrt{\pi}(\bar{\gamma})^{G_{d_{\text{SD}}}+G_{d_{\text{SRD}}}}\Gamma(G_{d_{\text{SD}}}+G_{d_{\text{SRD}}}+1)} + o\left(\bar{\gamma}^{-(G_{d_{\text{SD}}}+G_{d_{\text{SRD}}}+1)}\right), \quad (51)$$

By substituting corresponding values of Ω_{SD}, Ω_{SRD}, $G_{d_{\text{SD}}}$, and $G_{d_{\text{SRD}}}$ given in (49) and (10a) into (50), the desired result can be obtained as in (22a).

APPENDIX VI
CAPACITY BOUND

This section presents the sketches of the proof of C_{OPRA} (23). In order to obtain the closed-form capacity bound, a commonly used and mathematically tractable e2e SNR minimum upper bound is used. Let $\gamma_{eq} \leq \gamma_{eq}^{ub} = \min(\gamma_1, \gamma_2)$. Then the PDF of γ_{eq}^{ub} is given by

$$f_{\gamma_{eq}^{ub}}(x) = \sum_{a,b,c,k,l,m} \frac{d_1(a,b)d_2(k,l)(\phi x - (c+m))\,x^{c+m-1}}{a^{-c}k^{-m}\,(c)!\,(m)!\gamma_0^{-(c+m+1)}\bar{\gamma}_1^{c}\bar{\gamma}_2^{m}}\mathrm{e}^{-\phi x}, \quad (52)$$

where $\sum_{a,b,c,k,l,m}$ and ϕ are defined in (23). Now, C_{OPRA} in (23) can be derived by substituting (52) into $C_{\text{OPRA}} = \frac{B}{2\ln(2)}\int_{\gamma_0}^{\infty}\ln(x/\gamma_0)\,f_{\gamma_{eq}^{ub}}(x)\,\mathrm{d}x$ and solving the resulting integral by using [30, Eq. (3.381.3)]. The optimal cutoff SNR γ_0 satisfies $\int_{\gamma_0}^{\infty}(1/\gamma_0 - 1/x)f_{\gamma_{eq}^{ub}}(x)\,\mathrm{d}x = 1$ and can be evaluated as $1/\gamma_0\bar{F}_{\gamma_{eq}^{ub}}(\gamma_0) - \int_{\gamma_0}^{\infty}1/x f_{\gamma_{eq}^{ub}}(x)\,\mathrm{d}x = 1$, where $\int_{\gamma_0}^{\infty}1/x f_{\gamma_{eq}^{ub}}(x)\,\mathrm{d}x$ is evaluated by using [17, (3.351.2)] as in (53), where $\sum_{a,b,k,l}, \Theta_1, \Theta_2, \Theta_3$ and Θ_4 are defined in (24). $\bar{F}_{\gamma_{eq}^{ub}}(\gamma_0)$ is the complementary CDF evaluated at γ_0 and given by

$$\bar{F}_{\gamma_{eq}^{ub}}(\gamma_0) = \sum_{a,b,c,k,l,m} \frac{d_1(a,b)d_2(k,l)\gamma_0^{c+m+1}a^c k^m}{(c)!\,(m)!\bar{\gamma}_1^{c}\bar{\gamma}_2^{m}}\gamma_0^{c+m}\mathrm{e}^{-\phi\gamma_0}, \quad (54)$$

where $\sum_{a,b,c,k,l,m}$ is defined in (23). Now, γ_0 can be estimated efficiently by using (53) and (54), and a simple numerical technique such as the Bisection method.

APPENDIX VII
SUM CAPACITY OF MULTIUSER MIMO RELAY NETWORKS WITHOUT USER SCHEDULING

In order to derive the sum capacity in closed-form, the marginal PDFs of ordered eigenvalues, $\lambda_l|_{l=1}^{L}$, in (30) are required. However, $f_{\lambda_l}(x)$ of generalized $N \times N$ Wishart matrix are heavily involved [36], and hence, may not render compact closed-form expression for the sum capacity. Thus, a specific system set-up (i.e., $N_s = 3$, $N_r = 3$ and $L = 2$) is considered.

The joint PDF of the ordered eigenvalues of 3×3 Wishart matrix $\mathbf{H}_1\mathbf{H}_1^H$ is given by [36]

$$f_{\lambda_1,\lambda_2,\lambda_3}(\lambda_1,\lambda_2,\lambda_3) = \frac{1}{2}\mathrm{e}^{-(\lambda_1+\lambda_2+\lambda_3)}(\lambda_1-\lambda_2)^2(\lambda_1-\lambda_3)^2 \times (\lambda_2-\lambda_3)^2, \quad \text{where} \quad \lambda_1 \geq \lambda_2 \geq \lambda_3. \quad (55)$$

The marginal PDFs of λ_3, λ_2 and λ_1 are derived as

$$f_{\lambda_3}(x) = \int_x^{\infty}\int_{\lambda_2}^{\infty} f_{\lambda_1,\lambda_2,\lambda_3}(\lambda_1,\lambda_2,x)\,\mathrm{d}\lambda_1\mathrm{d}\lambda_2 = 3\mathrm{e}^{-3x}, \quad (56)$$

$$f_{\lambda_2}(x) = \int_0^{x}\int_{\lambda_2}^{\infty} f_{\lambda_1,\lambda_2,\lambda_3}(\lambda_1,x,\lambda_3)\,\mathrm{d}\lambda_1\mathrm{d}\lambda_3 = -6\mathrm{e}^{-3x} + \mathrm{e}^{-2x}\left[6 - 6x + 3x^2 + x^3 + x^4/2\right], \quad (57)$$

$$f_{\lambda_1}(x) = \int_0^{x}\int_0^{\lambda_2} f_{\lambda_1,\lambda_2,\lambda_3}(x,\lambda_2,\lambda_3)\,\mathrm{d}\lambda_3\mathrm{d}\lambda_2 = 3\mathrm{e}^{-3x} - \mathrm{e}^{-2x}\left[6 - 6x + 3x^2 + x^3 + x^4/2\right] + \mathrm{e}^{-x}\left[3 - 6x + 6x^2 - 2x^3 + x^4/4\right], \quad (58)$$

The sum capacity is then derived by using $C = \sum_{l=1}^{2}\int_0^{\infty}\log_2(1+x)/(2\bar{\gamma}_{eq})f_{\lambda_l}(x/\bar{\gamma}_{eq})\,\mathrm{d}x$ as given in (31).

REFERENCES

[1] Y. Yang *et al.*, "Relay technologies for WiMAX and LTE-advanced mobile systems," *IEEE Commun. Mag.*, vol. 47, no. 10, pp. 100–105, Oct. 2009.

[2] K. Loa *et al.*, "IMT-advanced relay standards," *IEEE Commun. Mag.*, vol. 48, no. 8, pp. 40–48, Aug. 2010.

[3] P. Dighe, R. Mallik, and S. Jamuar, "Analysis of transmit-receive diversity in Rayleigh fading," *IEEE Trans. Commun.*, vol. 51, no. 4, pp. 694–703, Apr. 2003.

[4] R. H. Y. Louie, Y. Li, and B. Vucetic, "Performance analysis of beamforming in two hop amplify and forward relay networks," in *Proc. 2008 IEEE Int. Conf. Commun.*, pp. 4311–4315.

[5] R. H. Y. Louie *et al.*, "Performance analysis of beamforming in two hop amplify and forward relay networks with antenna correlation," *IEEE Trans. Wireless Commun.*, vol. 8, no. 6, pp. 3132–3141, June 2009.

[6] T. Duong, H.-J. Zepernick, and V. Bao, "Symbol error probability of hop-by-hop beamforming in Nakagami-m fading," *Electron. Lett.*, vol. 45, no. 20, pp. 1042–1044, Sep. 2009.

[7] D. da Costa and S. Aissa, "Cooperative dual-hop relaying systems with beamforming over Nakagami-m fading channels," *IEEE Trans. Wireless Commun.*, vol. 8, no. 8, pp. 3950–3954, Aug. 2009.

[8] H. A. Suraweera, H. K. Garg, and A. Nallanathan, "Beamforming in dual-hop fixed gain relay systems with antenna correlation," in *Proc. 2010 IEEE Int. Conf. Commun.*, pp. 1–5.

[9] J.-B. Kim and D. Kim, "Performance of dual-hop amplify-and-forward beamforming and its equivalent systems in Rayleigh fading channels," *IEEE Trans. Commun.*, vol. 58, no. 3, pp. 729–732, Mar. 2010.

[10] H. Min *et al.*, "Effect of multiple antennas at the source on outage probability for amplify-and-forward relaying systems," *IEEE Trans. Wireless Commun.*, vol. 8, no. 2, pp. 633–637, Feb. 2009.

[11] H. Suraweera *et al.*, "Effect of feedback delay on downlink amplify-and-forward relaying with beamforming," in *Proc. 2009 IEEE Global Telecommun. Conf.*, pp. 1–5.

[12] B. Khoshnevis, W. Yu, and R. Adve, "Grassmannian beamforming for MIMO amplify-and-forward relaying," *IEEE J. Sel. Areas Commun.*, vol. 26, no. 8, pp. 1397–1407, Oct. 2008.

[13] X. Tang and Y. Hua, "Optimal design of non-regenerative MIMO wireless relays," *IEEE Trans. Wireless Commun.*, vol. 6, no. 4, pp. 1398–1407, Apr. 2007.

[14] C.-B. Chae *et al.*, "MIMO relaying with linear processing for multiuser transmission in fixed relay networks," *IEEE Trans. Signal Process.*, vol. 56, no. 2, pp. 727–738, Feb. 2008.

[15] I. Hammerstrom and A. Wittneben, "Power allocation schemes for amplify-and-forward MIMO-OFDM relay links," *IEEE Trans. Wireless Commun.*, vol. 6, no. 8, pp. 2798–2802, Aug. 2007.

[16] C. Song, K.-J. Lee, and I. Lee, "Performance analysis of amplify-and-forward spatial multiplexing MIMO relaying systems," in *Proc. 2010 IEEE Int. Conf. Commun.*, pp. 1–5.

[17] I. Gradshteyn and I. Ryzhik, *Table of Integrals, Series, and Products*, 7th edition. Academic Press, 2007.

[18] M. Abramowitz and I. Stegun, *Handbook of Mathematical Functions*. Dover Publications, Inc., 1970.

[19] J. N. Laneman, D. N. C. Tse, and G. W. Wornell, "Cooperative diversity in wireless networks: efficient protocols and outage behavior," *IEEE Trans. Inf. Theory*, vol. 50, no. 12, pp. 3062–3080, Dec. 2004.

$$\int_{\gamma_0}^{\infty}\frac{1}{x}f_{\gamma_{eq}^{ub}}(x)\mathrm{d}x=\sum_{a,b,k,l}\Bigg(\Theta_1 E_1(\phi\gamma_0)-\sum_{c=1}^{b}\Theta_2\phi^{1-c}(c\Gamma(c-1,\phi\gamma_0)\ -\Gamma(c,\phi\gamma_0))-\sum_{m=1}^{l}\Theta_3\phi^{1-m}\left(m\Gamma(m-1,\phi\gamma_0)-\Gamma(m,\phi\gamma_0)\right) \quad (53)$$
$$\times\sum_{c=1}^{b}\sum_{m=1}^{l}\Theta_4\phi^{1-c-m}((c+m)\Gamma(c+m-1,\phi\gamma_0)-\Gamma(c+m,\phi\gamma_0))\Bigg),$$

[20] E. Au *et al.*, "Analytical performance of MIMO-SVD systems in Ricean fading channels with channel estimation error and feedback delay," *IEEE Trans. Wireless Commun.*, vol. 7, no. 4, pp. 1315–1325, Apr. 2008.

[21] S. Zhou and G. Giannakis, "Adaptive modulation for multiantenna transmissions with channel mean feedback," *IEEE Trans. Wireless Commun.*, vol. 3, no. 5, pp. 1626–1636, Sep. 2004.

[22] Y. Chen and C. Tellambura, "Performance analysis of maximum ratio transmission with imperfect channel estimation," *IEEE Commun. Lett.*, vol. 9, no. 4, pp. 322–324, Apr. 2005.

[23] A. Maaref and S. Aissa, "Closed-form expressions for the outage and ergodic Shannon capacity of MIMO MRC systems," *IEEE Trans. Commun.*, vol. 53, no. 7, pp. 1092–1095, July 2005.

[24] Z. Wang and G. B. Giannakis, "A simple and general parameterization quantifying performance in fading channels," *IEEE Trans. Commun.*, vol. 51, no. 8, pp. 1389–1398, Aug. 2003.

[25] M. O. Hasna, "Average BER of multihop communication systems over fading channels," in *Proc. 2003 IEEE Int. Conf. Electron.*, vol. 2, pp. 723–726.

[26] G. Amarasuriya, C. Tellambura, and M. Ardakani, "Asymptotically-exact performance bounds of AF multi-hop relaying over Nakagami fading," *IEEE Trans. Commun.*, vol. 59, no. 4, pp. 962–967, Apr. 2011.

[27] M. McKay, A. Grant, and I. Collings, "Performance analysis of MIMO-MRC in double-correlated Rayleigh environments," *IEEE Trans. Commun.*, vol. 55, no. 3, pp. 497–507, Mar. 2007.

[28] A. Annamalai, C. Tellambura, and V. K. Bhargava, "Efficient computation of MRC diversity performance in Nakagami fading channel with arbitrary parameters," *Electron. Lett.*, vol. 34, no. 12, pp. 1189–1190, June 1998.

[29] T. Nechiporenko *et al.*, "On the capacity of Rayleigh fading cooperative systems under adaptive transmission," *IEEE Trans. Wireless Commun.*, vol. 8, no. 4, pp. 1626–1631, Apr. 2009.

[30] M.-S. Alouini and A. Goldsmith, "Capacity of Rayleigh fading channels under different adaptive transmission and diversity-combining techniques," *IEEE Trans. Veh. Technol.*, vol. 48, no. 4, pp. 1165–1181, July 1999.

[31] T. Yoo and A. Goldsmith, "On the optimality of multiantenna broadcast scheduling using zero-forcing beamforming," *IEEE J. Sel. Areas Commun.*, vol. 24, no. 3, pp. 528–541, Mar. 2006.

[32] H. Bolcskei, M. Borgmann, and A. J. Paulraj, "Impact of the propagation environment on the performance of space-frequency coded MIMO-OFDM," *IEEE J. Sel. Areas Commun.*, vol. 21, no. 3, pp. 427–439, Apr. 2003.

[33] M. O. Hasna and M. S. Alouini, "End-to-end performance of transmission systems with relays over Rayleigh-fading channels," *IEEE Trans. Wireless Commun.*, vol. 2, no. 6, pp. 1126–1131, Nov. 2003.

[34] S. Jin *et al.*, "Asymptotic SER and outage probability of MIMO MRC in correlated fading," *IEEE Signal Process. Lett.*, vol. 14, no. 1, pp. 9–12, Jan. 2007.

[35] Z. Wang and G. B. Giannakis, "A simple and general parameterization quantifying performance in fading channels," *IEEE Trans. Commun.*, vol. 51, no. 8, pp. 1389–1398, Aug. 2003.

[36] C. G. Khatri, "Distribution of the largest or the smallest characteristic root under null hypothesis concerning complex multivariate normal populations," *Ann. Math. Stat.*, vol. 35, pp. 1807–1810, Dec. 1964.

Gayan Amarasuriya (S'09) received the B.Sc. degree in Electronic and Telecommunication Engineering (with first-class honors) from the University of Moratuwa, Moratuwa, Sri Lanka, in 2006. He is currently working towards the Ph.D. degree at the Electrical and Computer Engineering Department, University of Alberta, AB, Canada. His research interests include design and analysis of new transmission strategies for cooperative MIMO relay networks and physical layer network coding.

Chintha Tellambura (SM'02-F'11) received the B.Sc. degree (with first-class honors) from the University of Moratuwa, Moratuwa, Sri Lanka, in 1986, the M.Sc. degree in electronics from the University of London, London, U.K., in 1988, and the Ph.D. degree in electrical engineering from the University of Victoria, Victoria, BC, Canada, in 1993.

He was a Postdoctoral Research Fellow with the University of Victoria (1993-1994) and the University of Bradford (1995-1996). He was with Monash University, Melbourne, Australia, from 1997 to 2002. Presently, he is a Professor with the Department of Electrical and Computer Engineering, University of Alberta. His research interests include Diversity and Fading Countermeasures, Multiple-Input Multiple-Output (MIMO) Systems and Space-Time Coding, and Orthogonal Frequency Division Multiplexing (OFDM).

Prof. Tellambura is an Associate Editor for the IEEE TRANSACTIONS ON COMMUNICATIONS and the Area Editor for Wireless Communications Systems and Theory in the IEEE TRANSACTIONS ON WIRELESS COMMUNICATIONS. He was Chair of the Communication Theory Symposium in Globecom'05 held in St. Louis, MO.

Masoud Ardakani (M'04-SM'09) received the B.Sc. degree from Isfahan University of Technology in 1994, the M.Sc. degree from Tehran University in 1997, and the Ph.D. degree from the University of Toronto, Canada, in 2004, all in electrical engineering. He was a Postdoctoral fellow at the University of Toronto from 2004 to 2005. He is currently an Associate Professor of Electrical and Computer Engineering and Alberta Ingenuity New Faculty at the University of Alberta, Canada, where he holds an Informatics Circle of Research Excellence (iCORE) Junior Research Chair in wireless communications. His research interests are in the general area of digital communications, codes defined on graphs and iterative decoding techniques. Dr. Adrakani serves as an Associate Editor for the IEEE TRANSACTIONS ON WIRELESS COMMUNICATIONS and the IEEE COMMUNICATION LETTERS.